*Research Article*

# A Novel Approach for Monitoring the Ecoenvironment of Alpine Wetlands using Big Geospatial Data and Cloud Computing

**Haijun Wang** [iD],[1,2] **Xiangdong Kong** [iD],[1,3] **Ji Luo,**[1] **Pengju Li,**[1] **Tianhui Xie,**[1] **Xiaobo Yi,**[1] **Fang Wang,**[1] **and Jie Xiao**[1]

[1]*School of Economics, Sichuan University of Science & Engineering, Zigong 643002, China*
[2]*College of Earth Science, Chengdu University of Technology, Chengdu 610059, China*
[3]*Faculty of Business Administration, Rajamangala University of Technology, Thanyaburi, Pathum Thani 12110, Thailand*

Correspondence should be addressed to Xiangdong Kong; kongxiangdong@suse.edu.cn

Alpine wetlands in western Sichuan plateau (WSCP) are located on the eastern edge of the Qinghai-Tibet Plateau (QTP), where the ecological environment is very sensitive to global climate change. Being naturally driven coupled with unreasonable human development activities, alpine wetlands have experienced serious ecological and environmental issues such as drought, inversion, and desertification. However, due to the limitations of data sources and calculation models, it is impossible for us to deeply understand the change mechanism and spatial difference of the ecological environment of the alpine wetland (EEAW) in previous studies. In view of this, an innovative approach for monitoring the EEAW change has been proposed in this paper. We employ the approach to perform the EEAW change trend analysis, and some meaningful characteristics were founded. Specifically, it includes the fol1owing aspects. The air temperature increase is relatively significant, while the precipitation change has obvious spatial differentiation, and even some region's precipitation experienced a decrease especially in plot1. In Haizishan, Lugu Lake, and Bari Lake, we explored an interesting phenomenon that the precipitation increases first and then decrease, and the turning point occurred around 1999. Increases in air temperature and evaporation have aggravated the drought in high-latitude areas. The drought situation has been alleviated in high-altitude areas due to the acceleration of snow melt water. Wetland vegetation and biomass presented an overall increasing trend, but the degradation also occurs in some area, including Zoige and Lugu Lake area. The human activity disturbances of wetland degradation mainly include the settlements expansion, agricultural development, and the ecotourism prosperity. Among them, targeted poverty alleviation projects have accelerated the urbanization in WSCP, and the development of agriculture and tourism has increased the interference of wetlands. Additionally, we have used Landsat images and national wetland survey data (1999, 2013, and 2020 year) from the past two decades to verify the EEAW trend and confirm the reliability of the analysis results using this approach.

## 1. Introduction

The global wetland area was about $5.7 \times 10^8 \, hm^2$ in 2015, and due to the unreasonable development, nearly 80% of the wetland resources are degrading or disappearing [1–3]. According to the Global Wetland Outlook (GWO) issued by the Ramsar Convention in 2018, the global wetland area decreased by 75% from 1975 to 2015, and wetland shrinkage accelerated after 2000. It is an indisputable fact that wetland ecosystem has become the most severely destroyed terrestrial ecosystem [4, 5]. In addition, according to the latest research results on wetlands by the Oxford University research team released by International Union for Conservation of Nature (IUCN) in August 2020, about 22.8% of the 500 wetlands surveyed worldwide have experienced a shrinkage since 2015, mostly in economically underdeveloped areas [6]. Therefore, we can see that wetland ecosystems are facing severe environmental threats on a global scale.

China's wetland area was about $5.36 \times 10^7 \, hm^2$ [7], accounting for about 9.4% of the world's wetland area. China joined the International Wetland Convention (IWC) in 1992; since then, it has conducted two national-scale wetland

resource surveys. The results of the survey show that the wetland area has decreased by $3.4 \times 10^6 \, \text{hm}^2$ from 2003 to 2013, with a reduction rate of 9.33%. The survey also showed that the environmental threats on wetlands have further increased, and the frequency of threats has increased by 38.71% [8]. The alpine wetland is an important wetland type in China, accounting for 41.2% of the national wetland area. It is mainly distributed in the Qinghai-Tibet Plateau (QTP), Yunnan-Guizhou Plateau (YGP), and Mongolia-Xinjiang Plateau (MXP). In order to better protect and scientifically develop alpine wetland resources, China wetland resources conservation association (CWRCA) established the alpine wetland protection professional committee (AWPPC) in Kunming in December 2019. It also reflects the importance and urgency of the alpine wetland ecosystem protection in western China.

Western Sichuan Plateau (WSCP) is located on the eastern edge of the QTP [9], with typical alpine meadows and unique alpine wetlands in the world [10, 11]. In this region, there is the largest swamp wetland of China-Zoige wetland [12], which accounts for 20% of China's wetland area [13]. The unique natural environment has bred a rich flora and fauna community, and it is also the last habitat of endangered animals, plants, and alpine fish species in China, such as alpine leek, miscanthus, and black-necked crane [14, 15]. Moreover, it is an area sensitive to global climate change and ecologically fragile [16–18]. Therefore, monitoring the ecological environment of the alpine wetland (EEAW) change in this region is meaningful to regional biodiversity conservation, geochemical cycling, climate regulation [3, 19], biological resource development, and economic development in ethnic regions. Both the national main function zone planning (NMFZP 2011) and the national land and space planning (NLAP 2020) define the alpine wetland distribution area in WSCP as a national ecological function zone (NEFZ). The ecological function zone of the alpine wetland in WSCP and the typical forest and biodiversity function zone in southwest Sichuan are of great significance to establish the national ecological security barrier in the western section of China.

The alpine wetlands (Natural wetlands) in WSCP include river wetlands, lake wetlands, swamp wetlands, and glacial wetlands. This article focuses on the study of alpine swamps and lake wetlands. The formation, development, and extinction of alpine wetlands are affected and controlled by its surrounding ecological environment, such as geology-topography, climate-hydrology, and human activities. Accordingly, the monitoring of the EEAW is helpful to predict the future change trend of the alpine wetlands. WSCP is located in a sensitive and ecologically fragile area of global climate change [16–18], and the climate change and human activities have made a negative impact on the changes of alpine wetlands. In some areas, drought, reverse succession, and desertification of alpine wetlands have occurred [20–22]. Therefore, it is necessary to monitor the ecological environment of alpine wetland, which plays an important role in the protection of alpine wetland.

In recent years, some scholars and organizations have carried out research on the ecological environment of alpine wetlands in WSCP and have achieved some results [23–28]. However, due to the restrictions of the diverse geographical environment, such as uneven hydrothermal conditions, scattered wetland distribution, and inefficient analysis model, some problems were not still solved in the research on the ecological environment change of the alpine wetland in WSCP. The specific problems unsolved are as follows: (1) relevant studies are mainly concentrated on a single scale (medium or small scale), using the wetland change characteristic of a typical plot to represent the variation of the EEAW in the whole region, resulting in a lack of macroscopic and comparable research. (2) WSCP is a farming-pastoral zone, with underdeveloped economy and few data observation sites. Previous research mainly relied on site observations (e.g., weather stations and hydrological stations), with single data sources and poor timeliness of data acquisition, which led to the systematicness and comprehensiveness of EEAW monitoring needs to be improved. (3) Multisource remote sensing is an important data source for wetland ecological change monitoring. Mass remote sensing data processing and spatial analysis model operation require a computer with strong computing power. Even if the computing power can be improved by building small workstations, the improvement is limited. Therefore, it can be seen that the traditional wetland ecological research scale, data collecting method, and data calculation model cannot meet the multiscale ecological environment monitoring of alpine wetland in the WSCP.

In view of this, an innovative EEAW monitoring approach is proposed. The main principles of the method include three aspects: integrate international open-source Earth science datasets to establish a more comprehensive EEAW change monitoring indicator system, according to the Indicators for Important Wetland Monitoring of China (IIWMC 2011) and Technical Standards for Wetland Ecological Risk-Benefit Assessment of China (TSWERBAC 2011). Construct a spatial statistical coupled model with multiple algorithms as the core. The model can perform multiscale and long-term series spatial raster analysis, such as remote sensing images and satellite-driven product sets. Use this model to efficiently conduct the processing, analysis and visualization of EEAW index system in Western Sichuan Plateau based on the cloud computing platform.

## 2. Study Area and Dataset

*2.1. Study Area.* WSCP (Figure 1) is a section of the eastern margin of the QTP and the Hengduan Mountains. It is mainly composed of the Ganzi-Aba plateau and the mountains of western Sichuan, with an average elevation of about 4000–4500 m. The regional climate is controlled by the continental climate in the west and the monsoon climate in the east. It belongs to the typical climate zone of the QTP. The main part of WSCP is north of the $0°$ isotherm (January), with an average annual temperature ranging from $-4°C$ to $8°C$. The spatial distribution of temperature is that the northwest plateau is lower than the northern plateau, lower than the central high mountain, and lower than the southern valley. Additionally, WSCP is located to the east of the
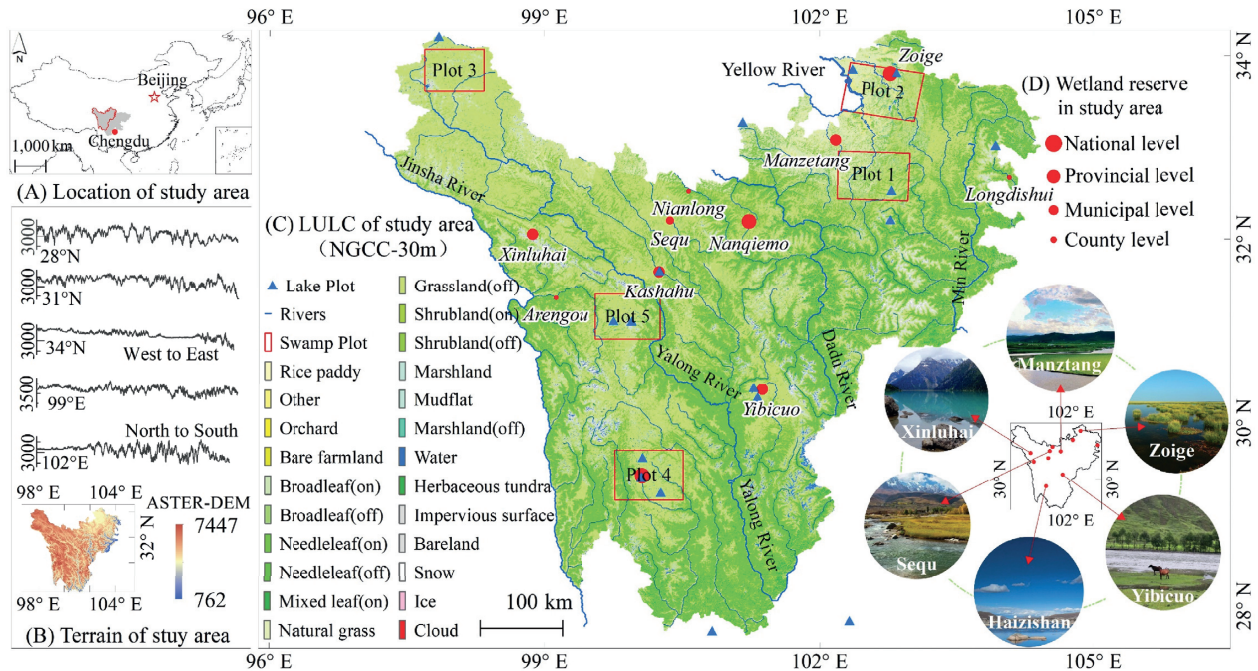
FIGURE 1: Geospatial feature of WSCP. (a) Location. (b) Terrain variation in latitudinal and meridional direction. (c) Land use and land cover. (d) Wetland nature reserve and its distribution.

geographic boundary of 400 mm precipitation. The annual precipitation ranges from 600 mm to 1000 mm. The precipitation is mainly concentrated from June to August, and it is higher in the east than in the west. The difference between dry and wet seasons is obvious and has a typical vertical zonal characteristic of climate. Moreover, this region is distributed in the upper reaches of the Yellow River hydrological area and Three Rivers hydrological area. The river network is densely distributed with some important water systems, such as the Yellow River, Jinsha River, Yalong River, Dadu River, and Min River. The largest alpine swamp belt (Zoige-Hongyuan-Aba area) in southern China is located here, and there are numerous plateau lakes (also known as little sea), forming a widespread alpine lake wetland in this region.

*2.2. Big Geospatial Data.* We used the GEE platform to integrate multisource remote sensing datasets and geographic databases from NASA, ESA, and USGS to establish a big geospatial dataset for monitoring the ecological environment of alpine wetlands (Table 1). The big geospatial dataset established contains 20 image products in five categories: wetland vegetation, wetland biomass, wetland hydrology, wetland climate, and human activities. Due to the obvious difference in the spatial and temporal resolution of the data, preprocessing was performed on the images. (1) Data resampling: the difference in data spatial resolution leads to poor comparability of analysis results. In view of the resolution of different image in the dataset and the geographic span of the study area, the dataset was resampled to 1000 m × 1000 m per pixel. (2) Data smoothing: long-term series data are easily affected by environmental factors,

which makes the image pixels have abnormal values in a certain period. We use S-G filter [29] to smooth the image dataset, so that the image values represent the real spectrum of ground objects. The whole process of data download, data preprocessing (resampling, smoothing, band combination, mosaic, and clipping), and data modeling and analyzing is completed by GEE platform.

## 3. Methodology

*3.1. Monitoring Index System.* With the impact of regional climate change and human activities (excessive grazing and tourism development), the ecological environment of this region has become fragile and sensitive. According to the natural environment, regional climatic conditions and economic development level in western Sichuan, as well as the focus of the research in this article, we refer to the IIWMC (2011) and the TSWERBAC (2011) to select 20 index factors to establish a EEAW monitoring index system of WSCP (Table 2). We use this monitoring indicator system to conduct the trend analysis of EEAW in western Sichuan.

*3.2. Computing and Analyzing Scale.* WSCP's alpine wetland includes swamp wetlands, lake wetlands, river wetlands, and glacial wetlands. The alpine wetland covers different latitudes and altitudes zones, and the wetland environment in different zones is obviously different. Different analysis scales will have a significant impact on the analysis results. Large-scale analysis can obtain the overall characteristics of wetland ecological environment changes, while small-scale analysis can better find the differences between different wetland plots. Accordingly, according to the spatial

TABLE 1: Geospatial big data collection used in this study.

| Id | Image collection | Sensor provider | Band | Code | Unit | Spatiotemporal resolution | | Type | Time series |
|---|---|---|---|---|---|---|---|---|---|
| 1 | SPOT vegetation | VGT\PROBA | Normalized difference vegetation index | NDVI | DN | 10-daily | 1 km | | 1998–2020 |
| 2 | NASA/GIMMS/3GV0 | AVHRR | Normalized difference vegetation index | NDVI | DN | 15-daily | 8 km | | 1981–2015 |
| 3 | MODIS/006/MOD13Q1 | MODIS | Normalized difference vegetation index | NDVI | DN | 16-daily | 250 m | Vegetation | 2000–2020 |
| 4 | MODIS/006/MCD43A4 | MODIS | Normalized difference vegetation index | NDVI | DN | daily | 500 m | | 2000–2020 |
| 5 | MODIS/006/MOD13Q1 | MODIS | Enhanced vegetation index | EVI | DN | 16-daily | 250 m | | 2000–2020 |
| 6 | MODIS/006/MOD15A2H | MODIS | FPAR_500 m | FPAR | Percent | 8-daily | 500 m | | 2000–2020 |
| 7 | MODIS/006/MOD17A2H | MODIS | Gross primary productivity | GPP | g*C/m$^2$ | 8-daily | 500 m | Biomass | 2000–2020 |
| 8 | MODIS/006/MOD17A3H | MODIS | Net primary productivity | NPP | g*C/m$^2$ | Yearly | 500 m | | 2001–2020 |
| 9 | MODIS/MCD43A4_006_NDWI | MODIS | Normalized difference water index | NDWI | DN | 16-daily | 500 m | | 2000–2020 |
| 10 | JRC/GSW1_1/Monthly history | OLI\ETM+ | Water | WAT | DN | Monthly | 30 m | | 1984–2018 |
| 11 | NOAA/CFSV2/FOR6H | NOAA/NEC | Soil moisture | SMO | % | 6-hourly | 0.2° | Hydrology | 1979–2020 |
| 12 | ECMWF/ERA5_LAND/MONTHLY | ECMWF | Snow_cover | SCO | % | Monthly | 0.1° | | 1979–2020 |
| 13 | ECMWF/ERA5_LAND/MONTHLY | ECMWF | Snow_depth | SDE | m | Monthly | 0.1° | | 1979–2020 |
| 14 | ECMWF/ERA5_LAND/MONTHLY | ECMWF | Temperature_2 m | ATP | K | Monthly | 0.1° | | 1979–2020 |
| 15 | ECMWF/ERA5_LAND/MONTHLY | ECMWF | Total precipitation | PRE | m | Monthly | 0.1° | | 1979–2020 |
| 16 | MODIS/006/MOD16A2 | MODIS | Evapotranspiration | ET | kg/m$^2$ | 8-daily | 500 m | Climate | 2001–2020 |
| 17 | MODIS/006/MOD11A2 | MODIS | Land surface temperature | LST | K | 8-daily | 1 km | | 2000–2020 |
| 18 | IDAHO_EPSCOR/TERRACLIMATE | Word Clim\JRA55 | Palmer drought severity index | PDSI | DN | Monthly | 2.5° | | 1958–2019 |
| 19 | DMSP-OLS/NIGHTTIME_LIGHTS | DMSP-OLS | Nightlight | NLI | DN | Yearly | 30″ | Human activity | 1992–2020 |
| 20 | WorldPop/GP/100 m/pop | World pop project | Population | POP | Person | Yearly | 3° | | 2000–2018 |

distribution characteristics of alpine wetlands and the quality of big geospatial dataset, multiscale analysis (Figure 2) is used to calculate the change trend of EEAW. Specifically, they are the regional scale (study area), the plot scale, and the site scale (circular buffer zone). On a regional scale, geospatial big dataset can be used to detect the change trend of EEAW from a macro perspective. Traditional observation method and single data are incomparable on such a large scope. The ecological environment change trend of each typical alpine wetland plot can be computed and analyzed by zoning. Compared with the regional scale, a more accurate change trend of EEAW can be acquired on a plot scale. Moreover, based on the site scale, we can reanalyze the data that have changed in some plots and get the variation characteristics at a finer level. According to the swamp wetland types and spatial distribution characteristics, we designed five sample plots in the study area; each plot is about 40 × 50 km (Figure 3). Plots cover the typical areas of the alpine swamp wetland in WSCP from low latitude to high latitude, such as Haizishan reserve, Xinglong, Zoige

reserve, Hongyuan, and Changsha reserve. Compared with the alpine swamp wetland, the distribution of lake wetland is more scattered. In order to more truly reflect the change trend of the ecological environment of different lake wetland, 18 typical lake wetland sample sites in WSCP were selected. The selection principle is that the environment of the lake wetland is representative, covering different latitudes and altitudes zone, including lakes of different sizes (0.5 km$^2$–45 km$^2$) and shapes, and the spatial distribution of sample sites is shown in Figure 1 (blue triangle symbol). We designed a circular buffer zone with a radius of 5 km and calculated the average value of the image in this circle region to represent the ecological environmental change of the lake wetland. When the lake is less than 5 km (width, length), we set the center of the circle to the lake center, when the lake is larger than 5 km, we set the center of the circle to the edge of the lake. The purpose is to avoid that the data calculation area is just lake water because the lake size is too large. Moreover, the lake wetlands mainly distribute on the high altitudes zone and human activities are

TABLE 2: Monitoring index system of EEAW in western plateau of Sichuan province.

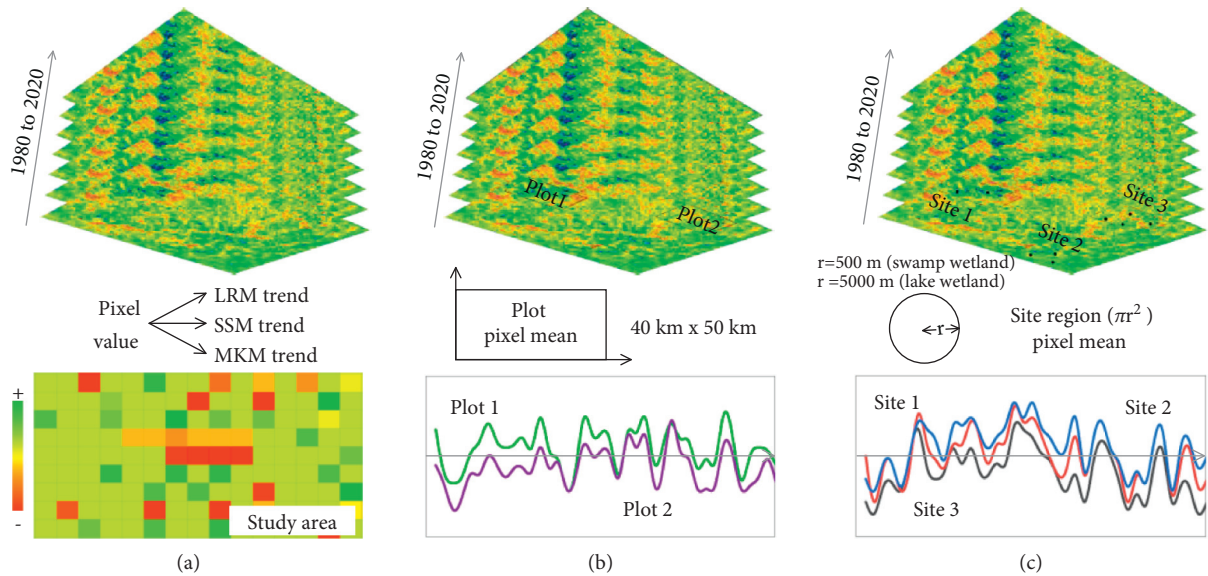| Environmental index | Subindex | Principle of index selection and its ecological analysis |
|---|---|---|
| Vegetation | GIMMS_NDVI SPOT_NDVI MOD_NDVI MOD_EVI | The swamp wetlands in the study area are dominated by swamp meadows. The vegetation coverage monitoring of the swamp wetlands can reflect the trend of wetland salinization and desertification. The occurrence of salinization and desertification indicates that the wetland ecological environment in this area has deteriorated. The vegetation index is a good remote sensing data product that represents the vegetation coverage; we select NDVI and EVI as the wetland vegetation monitoring indicator |
| Biomass | MOD_GPP MOD_NPP MOD_FPAR | Wetland vegetation productivity (GPP and NPP) and photosynthetically active radiation (FPAR) can better reflect the growth status and activity of wetland vegetation. The two indicators can reflect the ecological environment change of the wetland from another aspect |
| Hydrology | MOD_NDWI JRC_WAT NOAA_SMO ERA5_SCO ERA5_SDE | The water index is a remote sensing data product that can better reflect the distribution of surface water. Ice and snow melt water is an important water source for alpine wetlands. Snow cover and snow depth can reflect the wetland hydrological environment from the side, according to the regulations on wetland hydrology in GB/T 24708-2009. Combining the regional hydrological conditions of Ganzi and Aba prefectures and the availability of datasets, we selected the normalized water index (NDWI), water extent, surface soil moisture, and the thickness and area of ice and snow cover in the upstream area as the hydrological conditions of the alpine wetland monitoring indicators |
| Climate | ERA5_ATP ERA5_PRE MOD_ET MOD_LST IDAHO_PDSI | As an important part of the QTP, WSCP is sensitive to global climate change. Alpine wetland vegetation and hydrological changes are affected by climate change, so climate index is used as the ecological environment factors of alpine wetlands monitoring. We select the air temperature (ATP), precipitation (PRE), evaporation (ET), drought index (PDSI), and land surface temperature (LST) raster data |
| Human activity | WPP_POP NOAA_NLI | WSCP is an ecologically fragile area, and the alpine wetland is easily disturbed by human activity, especially population increase, residential expansion, and overgrazing. We use satellite-driven products, such as night light image, to represent population distribution and expansion |



FIGURE 2: Computing and analyzing principle of the geospatial big data collection in a multiscale. (a) Regional scale: grid of change trend in study area from 1980 to 2000. (b) Plot scale: curve of the factor in the plot from 1980 to 2020. (c) Site scale: curve of the factor in a representative site from 1980 to 2020.

rare, so the night-light index was not used when we analyzed the lake wetland environment change. The sample plot and sample site distribution, multiscale calculation principle, and the three-dimensional geographic environment of the sample plot are shown in Figures 1–3, respectively.

3.3. GEE Cloud Computing Platform. GEE [30] is a multiscale Earth science data analysis cloud computing platform, which includes databases, computing power, application program interface (API), and code views (Figure 4). Compared with European Earth Server [31] and Amazon Web Services [32], GEE has more plentiful geospatial data
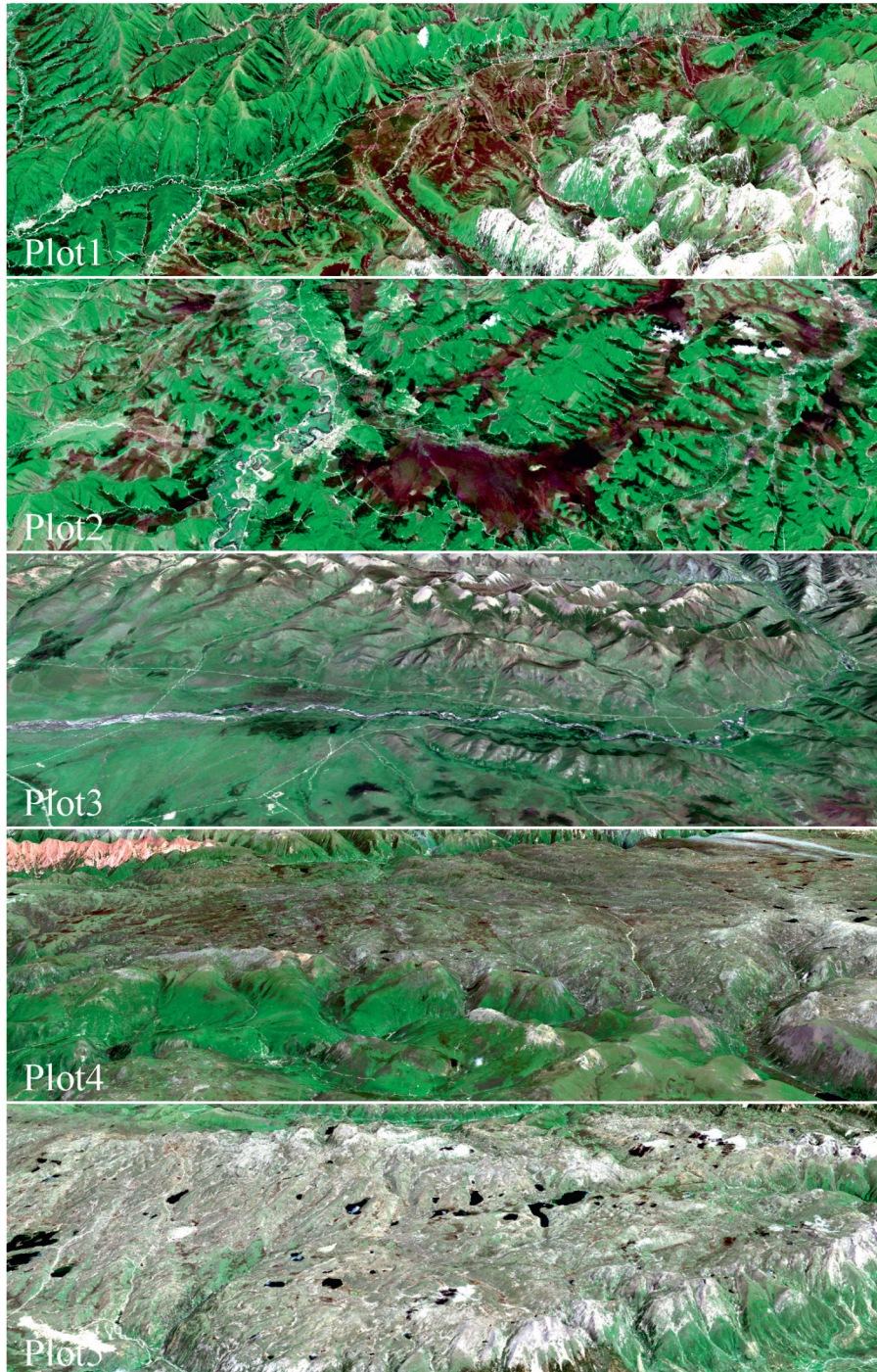
FIGURE 3: Three-dimensional geographical features of the alpine wetland plots selected.

sources, more diverse geospatial models and algorithms, and a more friendly graphical user interface (GUI). GEE integrates massive geospatial data resources, such as NASA Earth science database and ESA remote sensing dataset, to realize online acquisition, analysis, and visualization of multisource geospatial data. Real-time calculation and analysis of geospatial big data require a high-quality hardware support, especially the parallel computing power of GPU and CPU, and GEE has such a big computing power, which benefits from Google's long-term development of

information infrastructure [33]. GEE does not need to install application software when processing geospatial data. We can use Java script or Python to write programs through code view to invoke APIs to perform data processing and analysis.

*3.4. Trend Test Model.* This research mainly focuses on multiscale trend analysis of EEAW based on the big geospatial dataset (Table 1). According to the research needs,
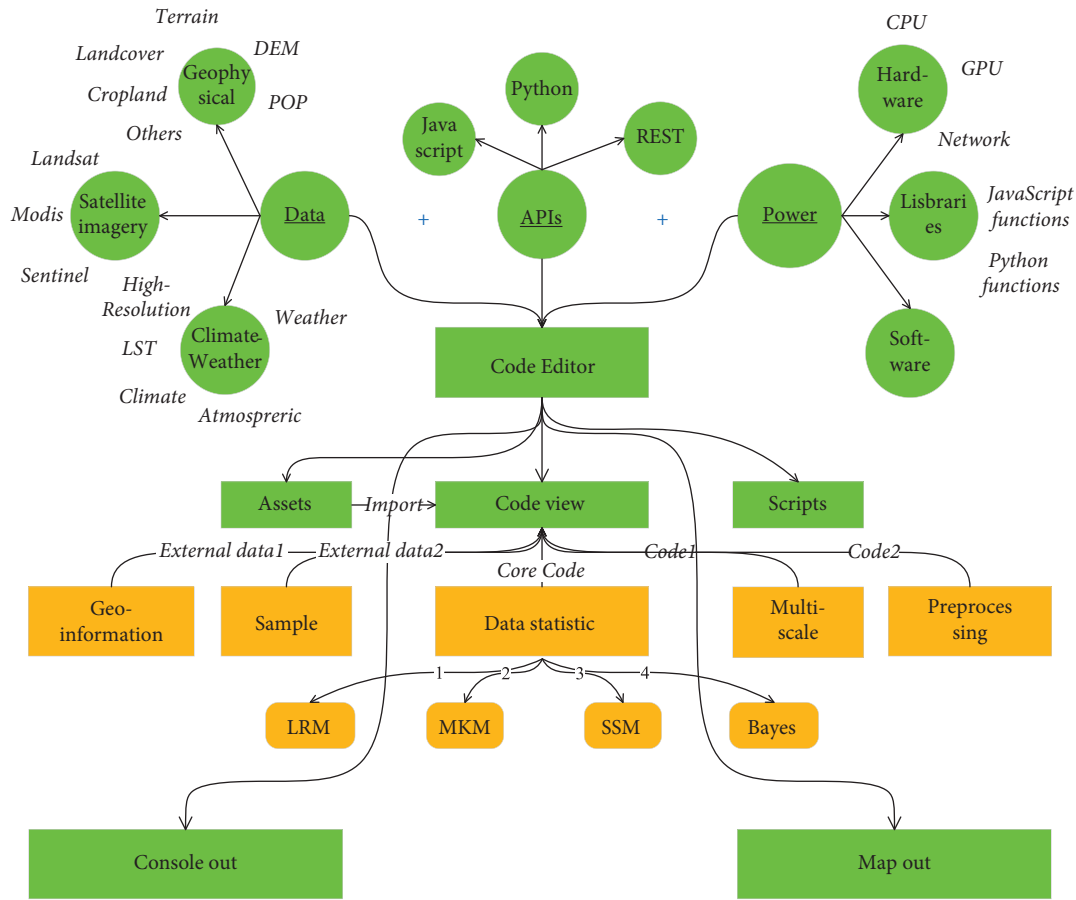
FIGURE 4: Integration principle of dataset, APIs, and computing power based on GEE platform in this study. The green rectangle is the GEE public sector, and the yellow rectangle is the author's personalized part.

three trend analysis models are selected. They are Linear Regression Model (LRM) [34–37], Mann-Kendall Model (MKM) [9, 38–41], and Sen's Slope Model (SSM) [42, 43]. The MKM model can be performed to detect the nonseasonal change trend (Monotonic trend) using image data (Discrete type), SSM model can quantitatively calculate the magnitude of the change trend and combine $Z$ statistics to test the significance of the change trend. Comparing with the numerical data, image data (Raster) computing needs more system memory when the MKM and SSM are running. To solve this problem, we used the LRM, which has the characteristics of simple structure and fast calculation, to assist the image computing of the MKM and SSM models. More specifically, the MKM and SSM are used to conduct spatiotemporal change trends analysis of EEAW based on the geospatial big data on a regional scale. A certain environment index dataset runs out of memory due to too long time series or high spatial resolution, and then we use the LRM model to perform trend analysis on this index dataset. For the trend analysis of the EEAW at the plot scale and site scale, we also use the LRM model to conduct it; the purpose is to use fully the computing power of GEE to improve the efficiency of geospatial big data analysis. The wetland classification data based on the multiperiod remote sensing image can also be used to validate the analysis results. The whole process of the geospatial big dataset analysis and

visualization is completed based the on the above four models using the GEE cloud computing platform.

## 4. Results

*4.1. Spatiotemporal Trend of Wetland Vegetation.* The seasonal changes of vegetation were analyzed in 5 swamp wetland plots and 18 lake wetland sites in WSCP; the results show that the 195th–230th day of the year (DOY) is the most vigorous period of vegetation activity. The phenological period of each plot is obviously different, and the time resolution of the geospatial dataset has the difference. We select the preprocessed GIMMS 3g, MODIS13Q1 NDVI, and EVI vegetation index from late June to mid-August of each year and calculate the average value of each data during this period. Temporal and spatial trend analyses of the average vegetation index were performed using the MKM, SSM, and LRM based on GEE cloud computing platform. Finally, the spatial-temporal change trend of the wetland vegetation in WSCP has been completed and acquired; the results are shown in Figures 5 and 6. It can be seen from Figure 6(c) that GIMMS 3g NDVI showed a weak growth trend (slope = 0.000032/decade) in the plot1 and plot2, and the NDVI experienced a weak downward trend in plot3 from 1982 to 2012. Through the analysis of the MODIS NDVI and EVI with the higher resolution (Figures 5(a) and
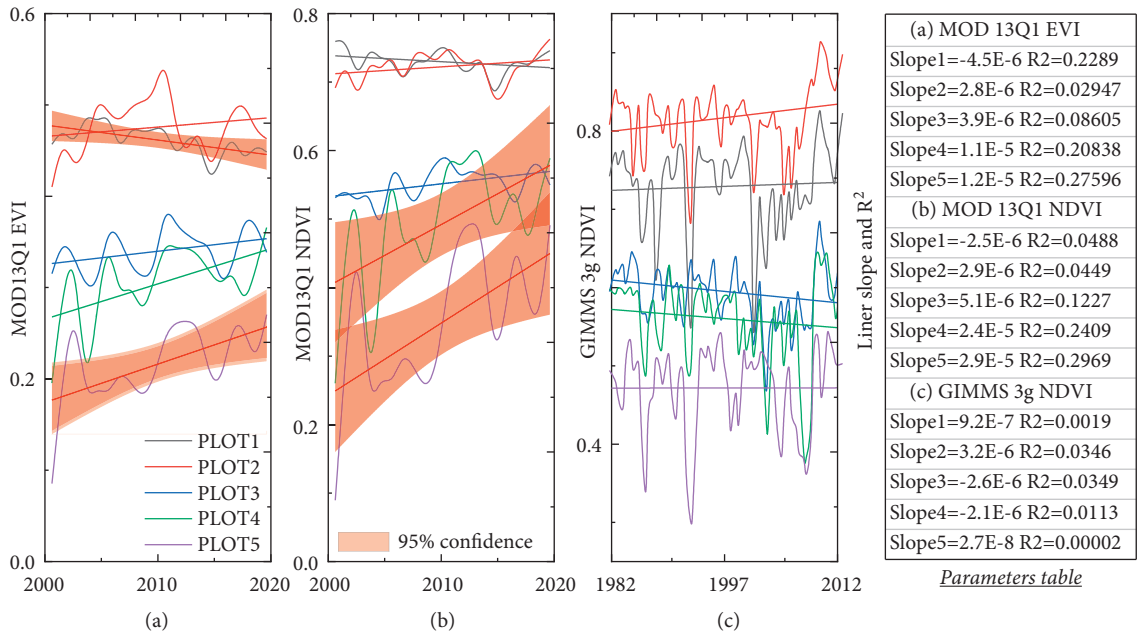
| | |
|---|---|
| (a) MOD 13Q1 EVI | |
| Slope1=-4.5E-6 R2=0.2289 | |
| Slope2=2.8E-6 R2=0.02947 | |
| Slope3=3.9E-6 R2=0.08605 | |
| Slope4=1.1E-5 R2=0.20838 | |
| Slope5=1.2E-5 R2=0.27596 | |
| (b) MOD 13Q1 NDVI | |
| Slope1=-2.5E-6 R2=0.0488 | |
| Slope2=2.9E-6 R2=0.0449 | |
| Slope3=5.1E-6 R2=0.1227 | |
| Slope4=2.4E-5 R2=0.2409 | |
| Slope5=2.9E-5 R2=0.2969 | |
| (c) GIMMS 3g NDVI | |
| Slope1=9.2E-7 R2=0.0019 | |
| Slope2=3.2E-6 R2=0.0346 | |
| Slope3=-2.6E-6 R2=0.0349 | |
| Slope4=-2.1E-6 R2=0.0113 | |
| Slope5=2.7E-8 R2=0.00002 | |

FIGURE 5: Vegetation change trend of the swamp wetland on a plot-scale. (a), (b), and (c) are the change trend of MOD13Q1 EVI (2000–2020), MOD13Q1 NDVI (2000–2020), and GIMMS 3g NDVI (1982–2012), respectively.
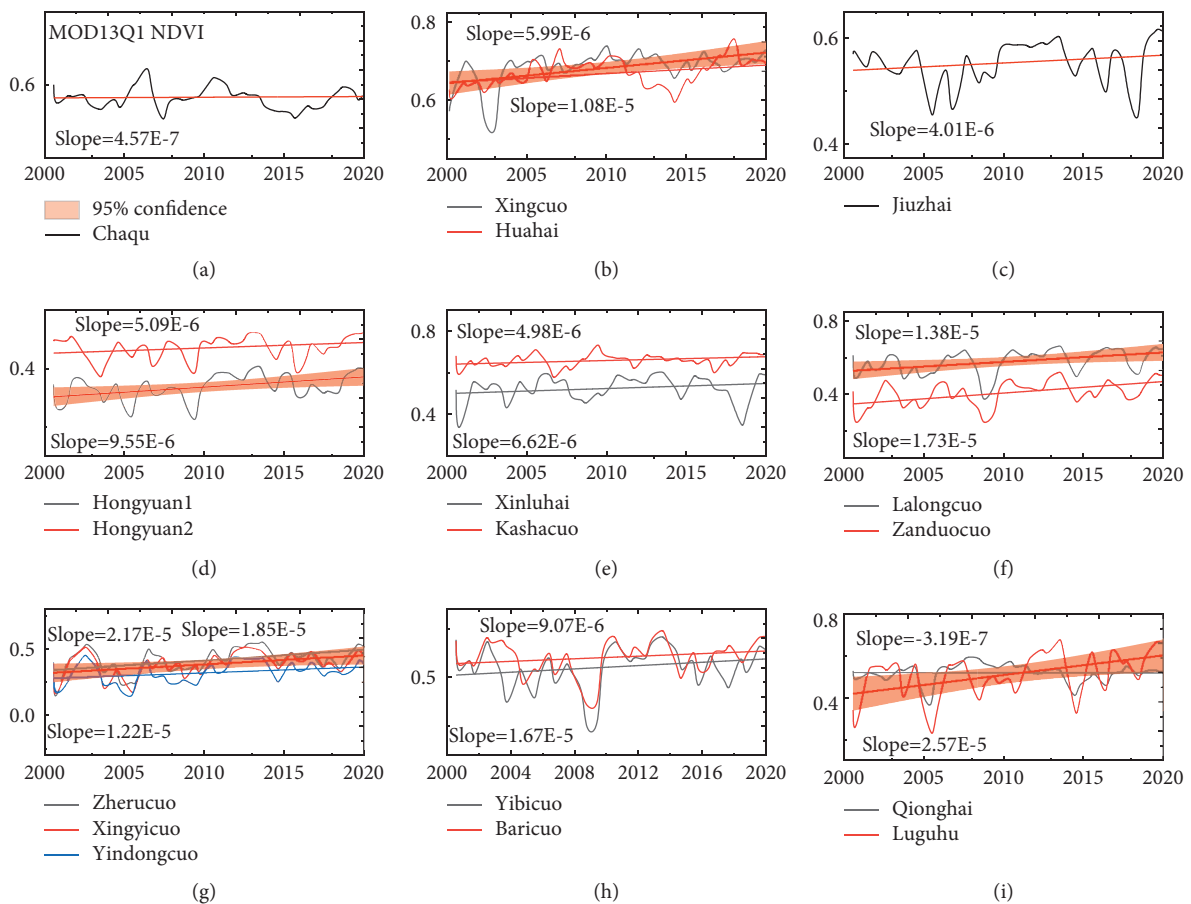


FIGURE 6: Vegetation change trend of the lake wetland on a site scale (2000–2020). Latitude of the lake site gradually decreased from subfigure (a) to (i). Elevation of sites (a), (d), (g), (f), and (h) are above 4500 m, elevation of sites (b), (c), and (e) is about 3000–3900 m, and elevation of site (i) is less than 3000 m.

5(b)), it is found that in the past 20 years, NDVI (slope = −0.0000025/decade) and EVI (slope = −0.0000045/ decade, $a = 0.05$) have appeared weak downward trend in plot1. Plot1 is located in the southern section of Hongyuan county, and its type belongs to the shrub swamp wetland. The data change trends in Figures 5(a) and 5(b) show that the vegetation degradation has occurred in this area. Plot2 distributed in Zoige county and its wetland type is herbaceous swamp. NDVI and EVI show an upward trend, and the slope is 0.0000029/decade and 0.0000028/decade, respectively. Both NDVI and EVI in Changsha Gongma Nature Reserve (Plot3) appeared an upward trend, with an increasing rate of 0.0000039/decade and 0.0000051/decade, respectively. It has the similar latitude with plot1, while the increasing trend rate was slower. The increasing trend of plot 4 and plot5 is more obvious than that of the other three plots, and the increasing rates of NDVI are 0.000021/decade years and 0.000029/decade ($a = 0.05$). The increasing trend of EVI is slower than that of NDVI, increasing at a rate of 0.000011/ decade and 0.000012/decade, respectively. As shown in Figure 6, the NDVI of alpine lake wetlands showed an increasing trend excepting Qionghai site. The NDVI of lake wetland in Haizishan area increased more significantly (Figure 6(g)), with an average growth rate of 0.000175/decade ($a = 0.05$), followed by Lalongcuo and Zanduocuo (Figure 7(f)) in the south of Xinglong county, with an average growth rate of 0.000105/decade. On the contrary, NDVI around Qionghai lake wetland (Figure 6(i)) has experienced a downward trend (slope = 3.19$E$−6/decade).

### 4.2. Spatiotemporal Trend of Wetland Biomass.

According to the IIWMC (2011) issued by the National Forestry and Grassland of China, wetland biomass is listed as an indicator for wetland ecological environment monitoring. Therefore, we use LRM, MKM, and SSM models to analyze the vegetation biomass satellite-driven product of alpine swamp wetlands, including MODIS FPAR, GPP, and NPP, to detect the change trend of wetland biomass in different plots in WSCP. FPAR reflects the productivity of wetland vegetation, and GPP and NPP indicate gross primary productivity and net primary productivity; they can reflect the vegetation growth status of the alpine wetland in western Sichuan. The calculation and analysis results of FPAR, GPP, and NPP in five plots are shown in Figure 7. It can be seen that the curves of the three wetland biomass parameters show an increasing trend. The FPAR increased obviously in the south of Xinglong county (Plot4), with a slope of 0.0148%/decade. FPAR change of Hongyuan (plot1) and Zoige (plot2) has similar trend characteristics. A significant increase trend of GPP happened in plot2 (slope = 0.2 g*C/m$^2$/decade, $a = 0.05$) and show a fluctuation characteristic during the GPP change process in plot5. It also reflects that the wetland environment is quite different in these two plots. Plot5 is located at the high altitude, with low temperature and sparse wetland vegetation, which is easily affected by surrounding environmental changes. The wetland vegetation in Zoige has a better climate and terrain condition, which makes GPP change less volatile. The average annual NPP change trend of

plots3 is 171.5 g*C/m$^2$/decade) slightly higher than plot1 and plot2 (Figure 7(c)). Through the analysis of wetland FPAR, GPP, and NPP, it can be seen that the vegetation biomass of the five plots shows an increasing trend, indicating that the vitality of wetland vegetation is relatively good.

We can see from the GPP curve of lake wetlands that the vitality of lake wetland vegetation experiences an increasing trend (Figure 8), which is generally consistent with the change trend of NDVI. The vegetation biomass of the Luguhu-Qionghai lake in the low latitude area and the Huahai lake wetland in the northern area is relatively high, and the GPP has shown a relatively rapid growth rate in the past 20 years. Compared with the spatial distribution of NDVI changes, the spatial distribution of GPP changes is also somewhat different. The rapid increase of GPP is mainly distributed in high latitude regions, such as Jiuzhaigou (0.18/ decade, $a = 0.05$), Zoige (0.18/decade, $a = 0.05$), and Hongyuan (0.14/decade, $a = 0.05$). The increase of NDVI and GPP also shows that the ecological environment of lake wetlands (5 km range) has an improvement, even if this upward trend is not obvious.

### 4.3. Spatiotemporal Trend of Wetland Climate.

All Earth surface processes, including the vegetation ecosystems succession, hydrological cycles, and carbon balance, are affected and controlled by climate change [44–46]. Accordingly, we integrate the ERA5 air temperature (ATP) and precipitation (PRE), IDAHO palmer drought severity index (PDSI), MODIS evapotranspiration (ET), and land surface temperature (LST) datasets and use the GEE cloud calculation platform to analyze the climate change trend in plot1–plot5. The analysis results of the climate factor change trend are shown in Figure 9. The change trend of ATP and PRE indicate that the air temperature and precipitation of the five plots experienced a regular change in the past 20 years (Figures 9(a) and 9(b)). Specifically, the temperature shows an upward trend, and it rises in high-latitude areas more obvious than that in low-latitude areas. The temperature rising rate of plot1 to plot5 is 0.00086 K/decade ($a = 0.05$), 0.00091 K/decade ($a = 0.05$), 0.00092 K/decade ($a = 0.05$), 0.00090 K/decade, and 0.00094 K/decade, respectively. The precipitation in plot1, plot2, and plot3 presents a decreasing trend, while this trend is weak (Figure 9(b)). The increase of temperature and the decrease of precipitation lead to the increase of surface water evaporation, which will cause to the shrinkage of wetland water area. The change curve of ET also proves this point (Figure 9(c)). Among the five plots, the ET in plot1, plot2, and plot3 showed a slight increase, and this trend was most obvious in plot2, with an increased rate of 0.00371 kg/m$^2$/ decade ($a = 0.05$). ET change trend is basically consistent with the air temperature change trend in the high-latitude plots (plot1, plot2, and plot3). While ET change trend shows a weak upward trend with a fluctuation in the low-latitude plots (plot4 and plot5). The PDSI of plot4 and plot5 showed a downward trend, with a decline rate of 0.73/decade and 0.89/decade, respectively, which was related to the increase of precipitation in these two plots. The increase in
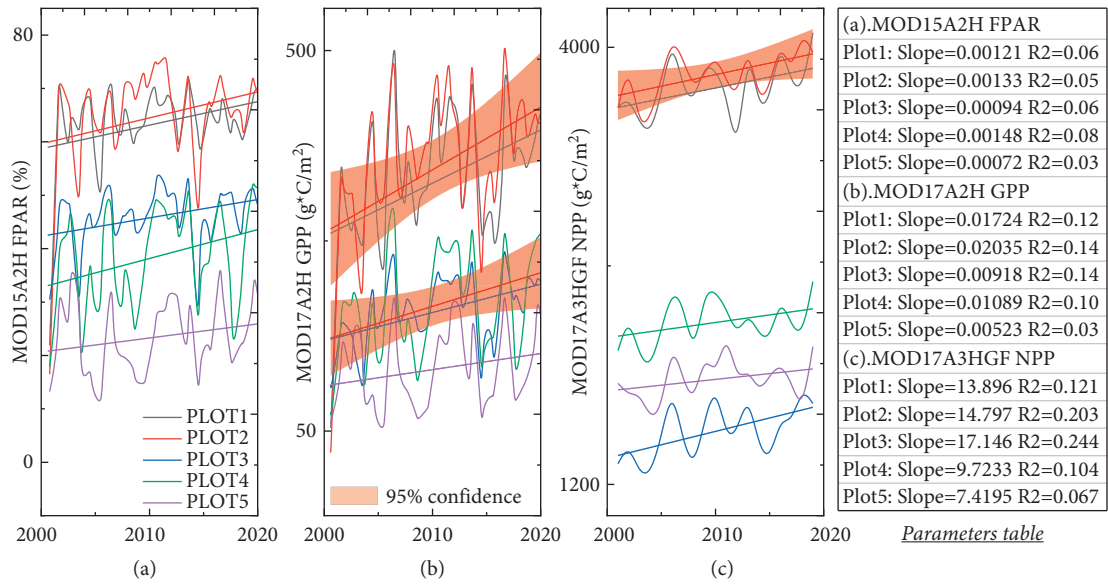
The parameters table shown in the figure:

| | |
|---|---|
| (a).MOD15A2H FPAR | |
| Plot1: Slope=0.00121 R2=0.06 | |
| Plot2: Slope=0.00133 R2=0.05 | |
| Plot3: Slope=0.00094 R2=0.06 | |
| Plot4: Slope=0.00148 R2=0.08 | |
| Plot5: Slope=0.00072 R2=0.03 | |
| (b).MOD17A2H GPP | |
| Plot1: Slope=0.01724 R2=0.12 | |
| Plot2: Slope=0.02035 R2=0.14 | |
| Plot3: Slope=0.00918 R2=0.14 | |
| Plot4: Slope=0.01089 R2=0.10 | |
| Plot5: Slope=0.00523 R2=0.03 | |
| (c).MOD17A3HGF NPP | |
| Plot1: Slope=13.896 R2=0.121 | |
| Plot2: Slope=14.797 R2=0.203 | |
| Plot3: Slope=17.146 R2=0.244 | |
| Plot4: Slope=9.7233 R2=0.104 | |
| Plot5: Slope=7.4195 R2=0.067 | |
| *Parameters table* | |

FIGURE 7: Biomass change trend of the swamp wetland on a plot scale. (a), (b), and (c) are the change trend of MOD15A2 FPAR (2000–2020), MOD17A2H GPP (2000–2020), and MOD17A3HGF NPP (2000–2020), respectively.
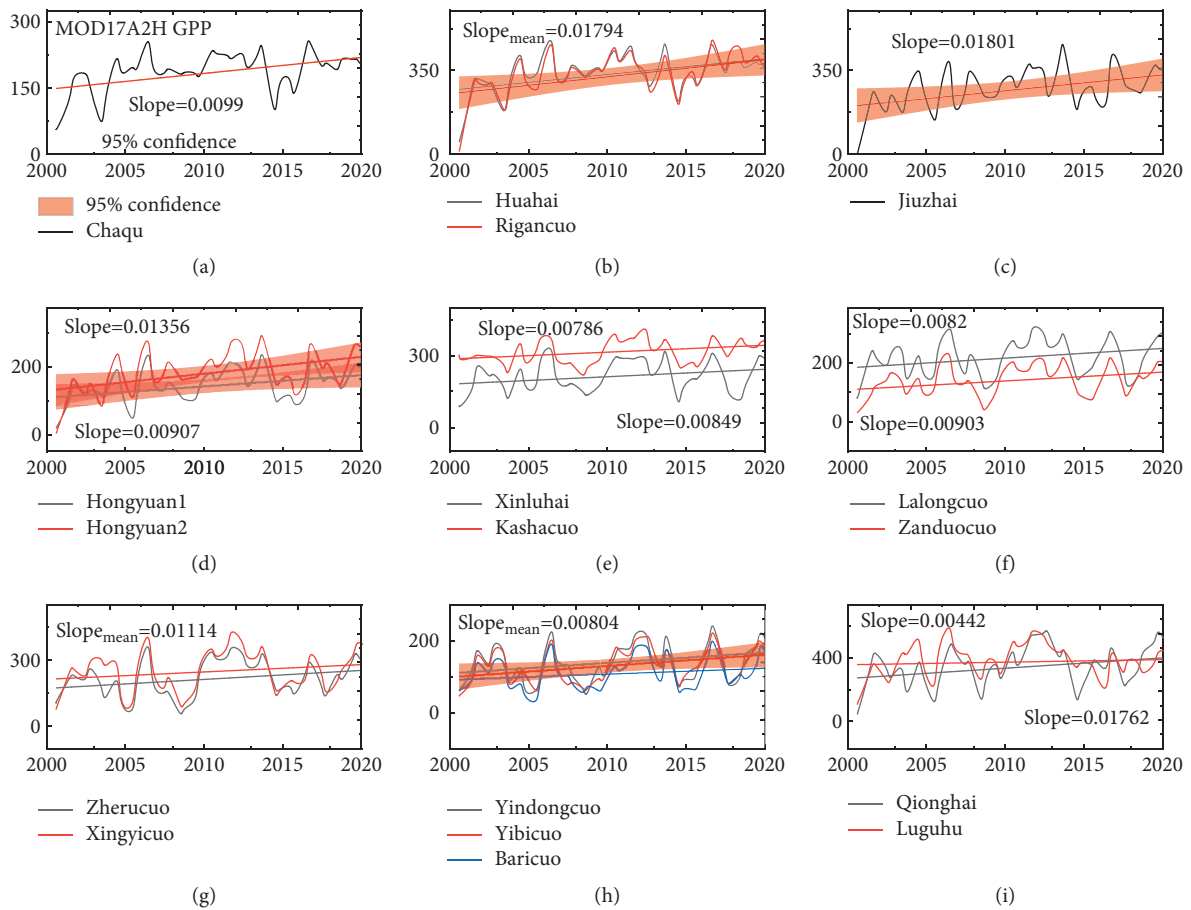


FIGURE 8: GPP change trend of the lake wetland on a site scale (2000–2020). The latitude of the lake site gradually decreased from subfigure (a) to (i). Elevation of sites (a), (d), (g), (f), and (h) are above 4500 m, elevation of sites (b), (c), and (e) are about 3000–3900 m, and elevation of site (i) is less than 3000 m.
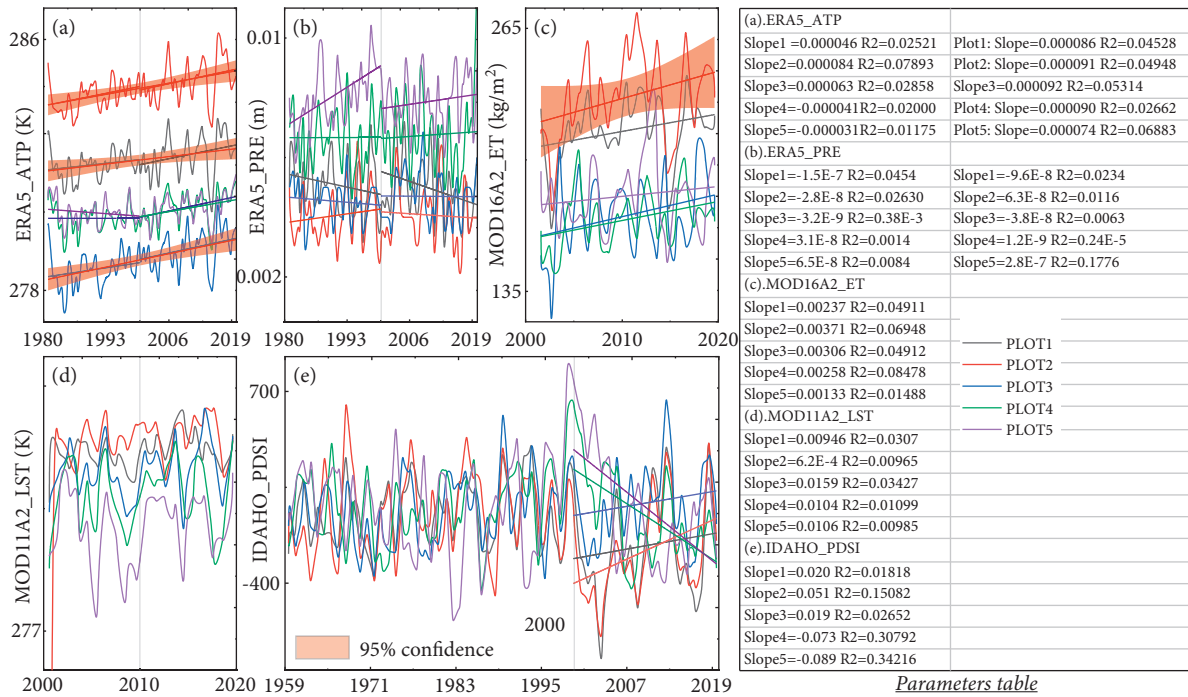
FIGURE 9: Climate change trend of the swamp wetland on a plot scale. (a), (b), (c), (d), and (e) is the change trend of ERA5 ATP (1980–2020), ERA5 PRE (1980–2020), MOD16A2 ET (2000–2020), MOD11A2 LST (2000–2020), and IDAHO PDSI (1959–2019), respectively.
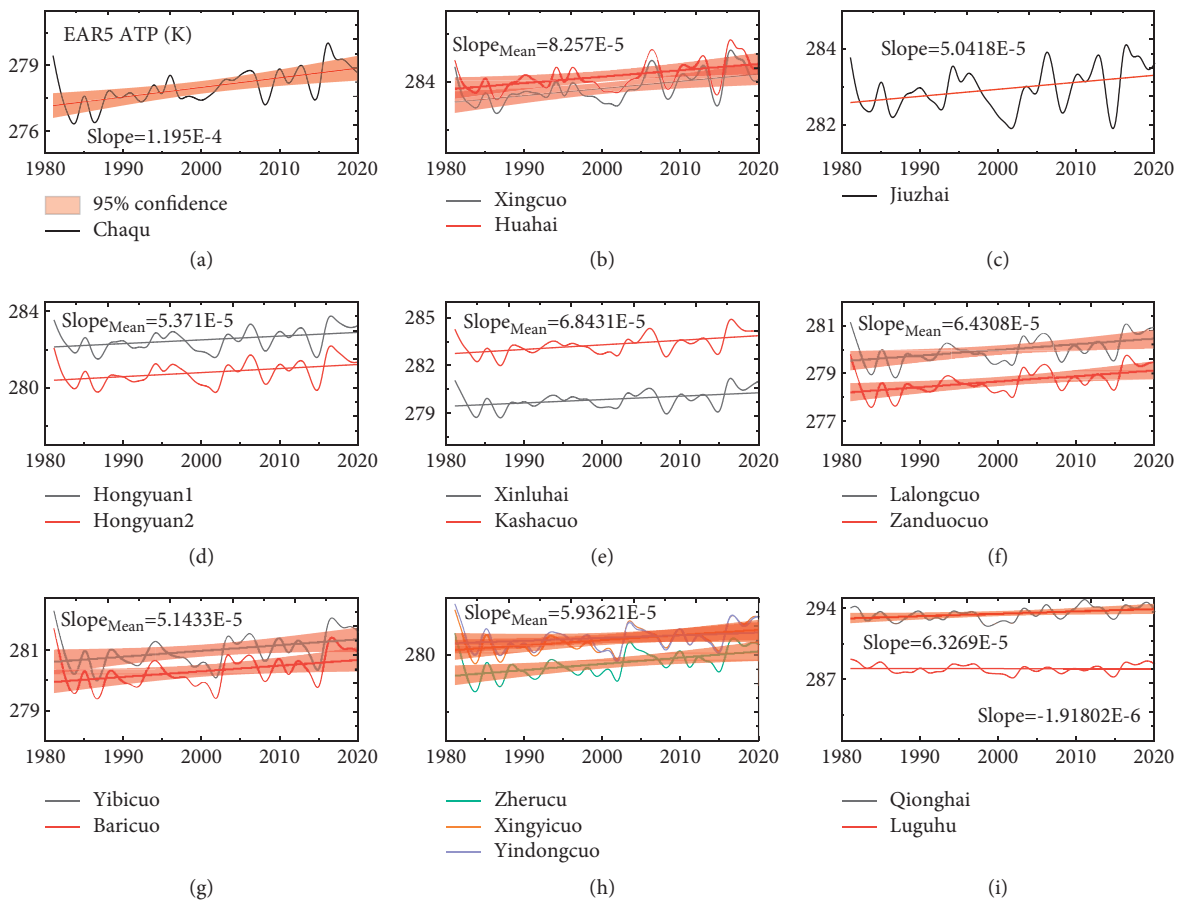


FIGURE 10: ATP change trend of the lake wetland on a site scale (1980–2020). Latitude of the lake site gradually decreased from subfigure (a) to (i). Elevation of sites (a), (d), (g), (f), and (h) are above 4500 m, elevation of sites (b), (c), and (e) are about 3000–3900 m, and elevation of site (i) is less than 3000 m.
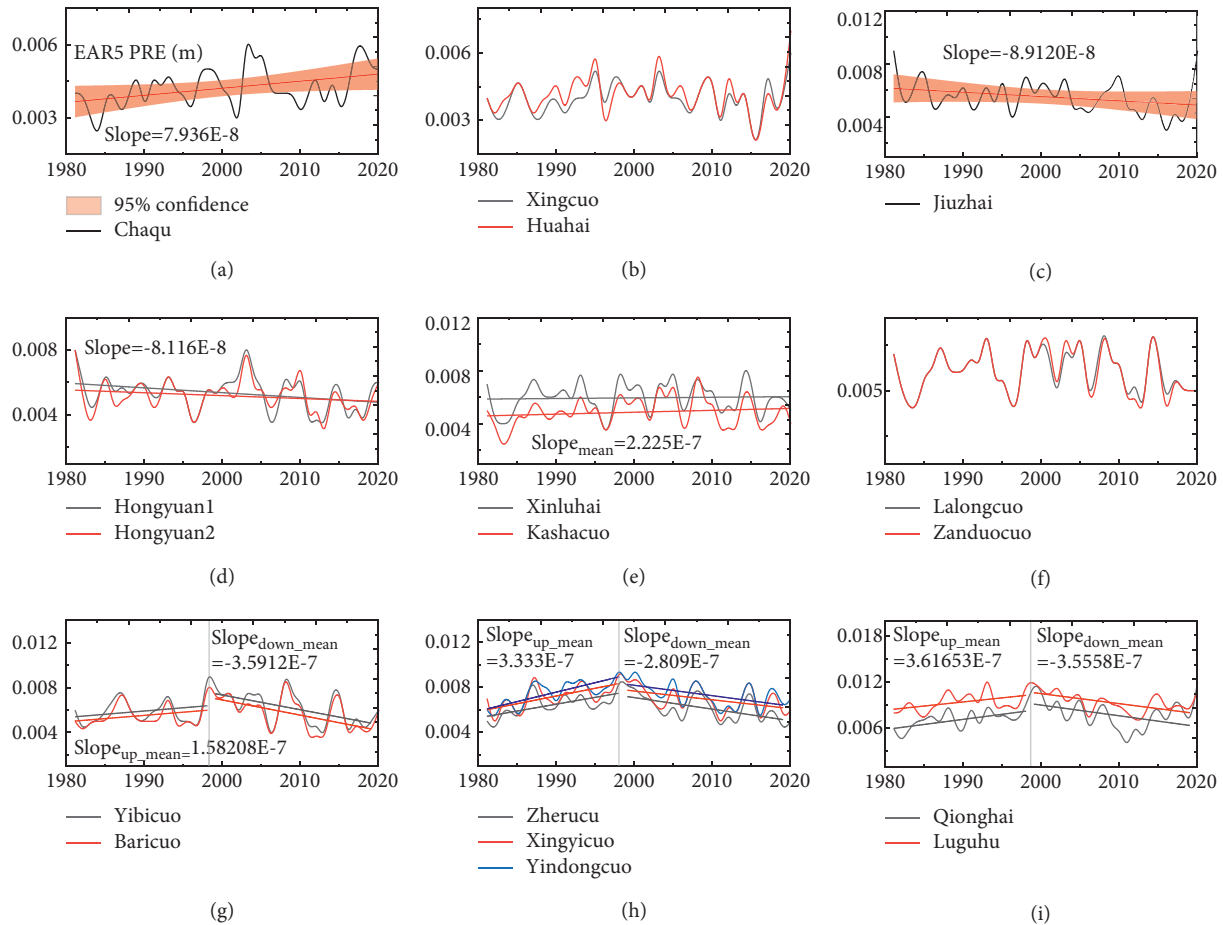
FIGURE 11: PRE change trend of the lake wetland on a site scale (1980–2020). Latitude of the lake site gradually decreased from subfigure (a) to (i). Elevation of sites (a), (d), (g), (f), and (h) are above 4500 m, elevation of sites (b), (c), and (e) are about 3000–3900 m, and elevation of site (i) is less than 3000 m.

temperature and decrease in precipitation in the three plots (plot1, plot2, and plot3) led to an increase in PDSI, which is reflected in Figure 9(e). In addition, the land surface temperature (LST) of the five plots showed a slight upward trend (Figure 9(d)).

The analysis of the air temperature and precipitation data of the typical alpine lake wetland sites in WSCP based on GEE cloud computing platform revealed the change trend and characteristics of the temperature and precipitation in the past 40 years (Figures 10 and 11). The temperature in the lake wetland distribution area showed an upward trend, and the temperature increase in high-latitude and high-altitude areas was more obvious. Among all lake wetland sample sites, the small lakes in the Chaco basin (slope = $1.195E - 3$/decade, $a = 0.05$), Xingcuo-Huahai in Zoige county (slope = $8.257E - 4$/decade, $a = 0.05$), Xinluhai-Kasha (slope = $6.848E - 4$/decade), and Lalongcuo-Zanduocuo (slope = $6.4308E - 4$/decade, $a = 0.05$) in southern Xinglong county have faster temperature increase rate (Figure 10). While in low-latitude and low-altitude region, the temperature has a downward trend, especially in Luguhu site (slope = $-1.9180E - 5$/decade). Compared with the change trend of temperature, the change characteristics of

precipitation has an obvious spatial difference in the geographical distribution. The precipitation in Chaco and Xinluhai-Kasha Lake wetland sites showed a weak increase trend, and the trend rates were $7.936E - 4$ mm/decade ($a = 0.05$) (Figure 11(a)) and $2.225E - 4$ mm/decade (Figure 11(e)). The change trends of precipitation in Xingcuo-Huahai, Yibi-Bari, Zheru-Xingyi-Yindong, Qionghai-Lugu Lake sites experience first increase and then decrease (Figures 11(g)–11(i)); this turning point of trend change is about 1998. In general, in the past 40 years, the temperature of the alpine lake wetland sites has shown an increasing trend and the change trend is more obvious in high-latitude region, while the precipitation has shown a decreasing trend, especially in the recent 20 years.

### 4.4. Spatiotemporal Trend of Wetland Hydrology. 
Earth surface water is the basis for the development of wetlands, and the surface water change will have an important impact on the ecological environment of wetlands. We integrated the international open-source water index (MOD43A4 NDWI), snow depth, snow cover (ERA5 SCO\SDE), and soil moisture (ERA5 SOIW) datasets to conduct surface water
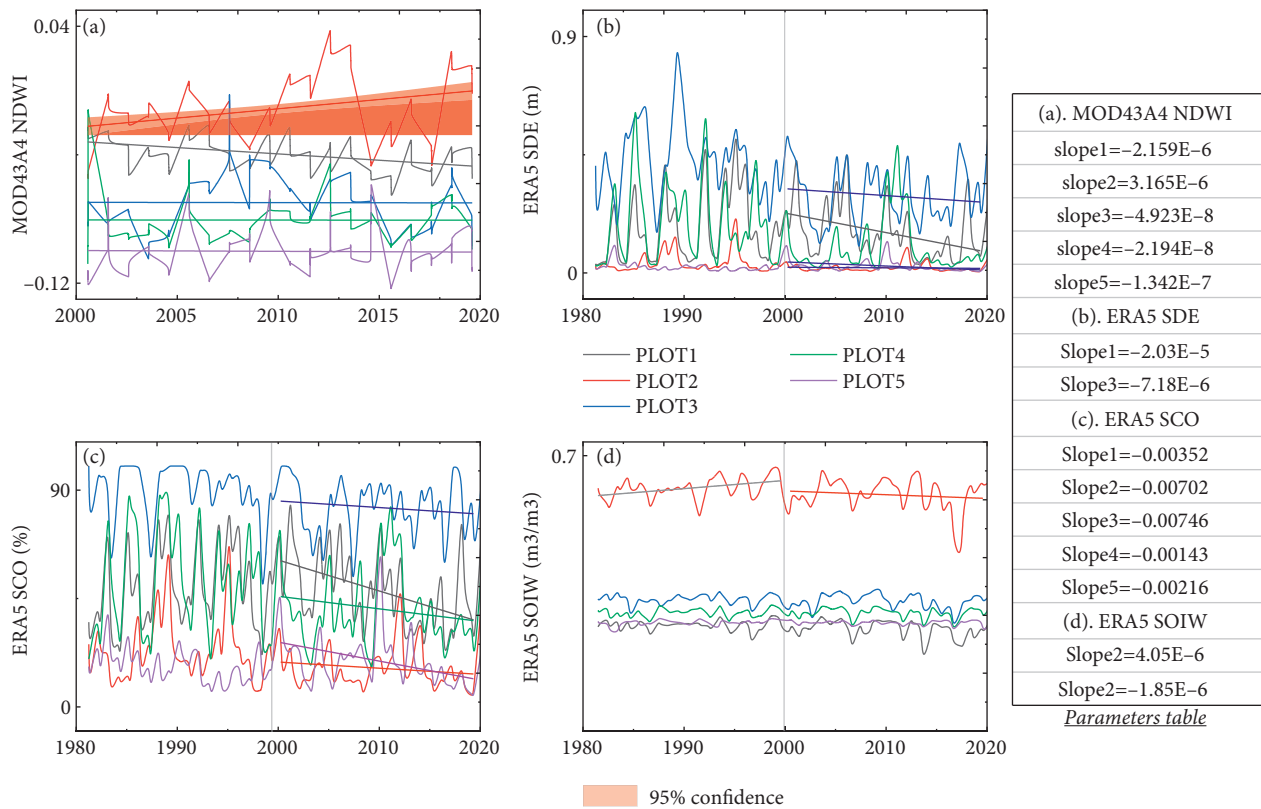
FIGURE 12: Hydrology change trend of the swamp wetland on a plot scale. (a), (b), (c), and (d) are the change trends of MOD43A4 NDWI (2000–2020), ERA5 SDE (1980–2020), ERA5 SCO (1980–2020), and ERA5 SOIW, respectively.

(Solid and liquid) change analysis of typical alpine swamp wetland plots (plot1 to plot5) in WSCP. Using the GEE platform and trend models to analyze the above five datasets, the temporal and spatial change characteristics of surface water and surface snow cover are obtained. Specifically, the results were shown in Figure 12. It can be seen that only the water index of the Zoige (slope = 0.0032%, $a = 0.05$) has a slight increase trend, while the other four plots have a slight decrease trend. The surface snow depth and cover of the 5 plots showed a decreasing trend, and the decreasing trend was the most obvious (slope = −0.035%/decade) in the southern part of Hongyuan (plot1). According to previous analyses, we found that the precipitation is increased in plot1, and the decrease of snow cover in this area indicates that the snow melting speed has accelerated. The change trend of surface soil moisture is not significant in WSCP; only there is a slight upward trend in the Zoige county.

Snow melt water is an important form of water supply for lake wetlands in high altitude areas. Analyzing the snow cover and depth of typical alpine lake wetland in western Sichuan can better monitor the hydrological environment. Through the analysis of snow cover and snow depth raster data in the past 40 years, the change trend of snow depth (SDE) and snow cover (SCO) of typical alpine lake wetlands in western Sichuan is obtained (Figures 13 and 14). The snow cover of the lake wetlands such as Chaco, Hongyuan, Xinluhai, and Zanduocuo is relatively large, and the fluctuation trend is relatively weak. By contrast, the snow covers of the alpine lake wetlands, including Xingcuo-Huahai,

Zheru-Xingyi, and Yibi-Bari, showed a decreasing trend, with a decreasing rate is −0.0155%/decade ($a = 0.05$), −0.0101%/decade, and −0.018%/decade ($a = 0.05$), respectively. The lake wetlands in Hongyuan, Xinluhai, and Lalongcuo-Zanduocuo have a high snow depth. The snow depth of Jiuzhai and Hongyuan lake wetlands increased first and then decreased. The turning points of the change trend were 1995 and 2005, respectively.

### 4.5. Spatiotemporal Trend of External Interference.

EEAW change is also affected and controlled by human activities, excepting the natural environment. Alpine wetlands in western Sichuan are distributed in the farming-pastoral zone, which is a typical ecologically fragile area. Human activities, such as the expansion of farming area, the extending of settlements, and the excessive development of tourism in some areas, will bring negative effects to the EEAW. Therefore, we analyzed the existing international open-source geospatial datasets that can reflect the scope and intensity of human activities on the Earth. We finally selected the night light data, population (POP) density grid, and land surface temperature (LST) data. Night lights and population density raster can reflect the expansion of residential areas and the characteristics of population spatial distribution. Agricultural farming can change the thermal properties of the land surface, especially in cold regions [47–50]. To some extent, LST data can be used to characterize the impact of agricultural farming on alpine wetlands.
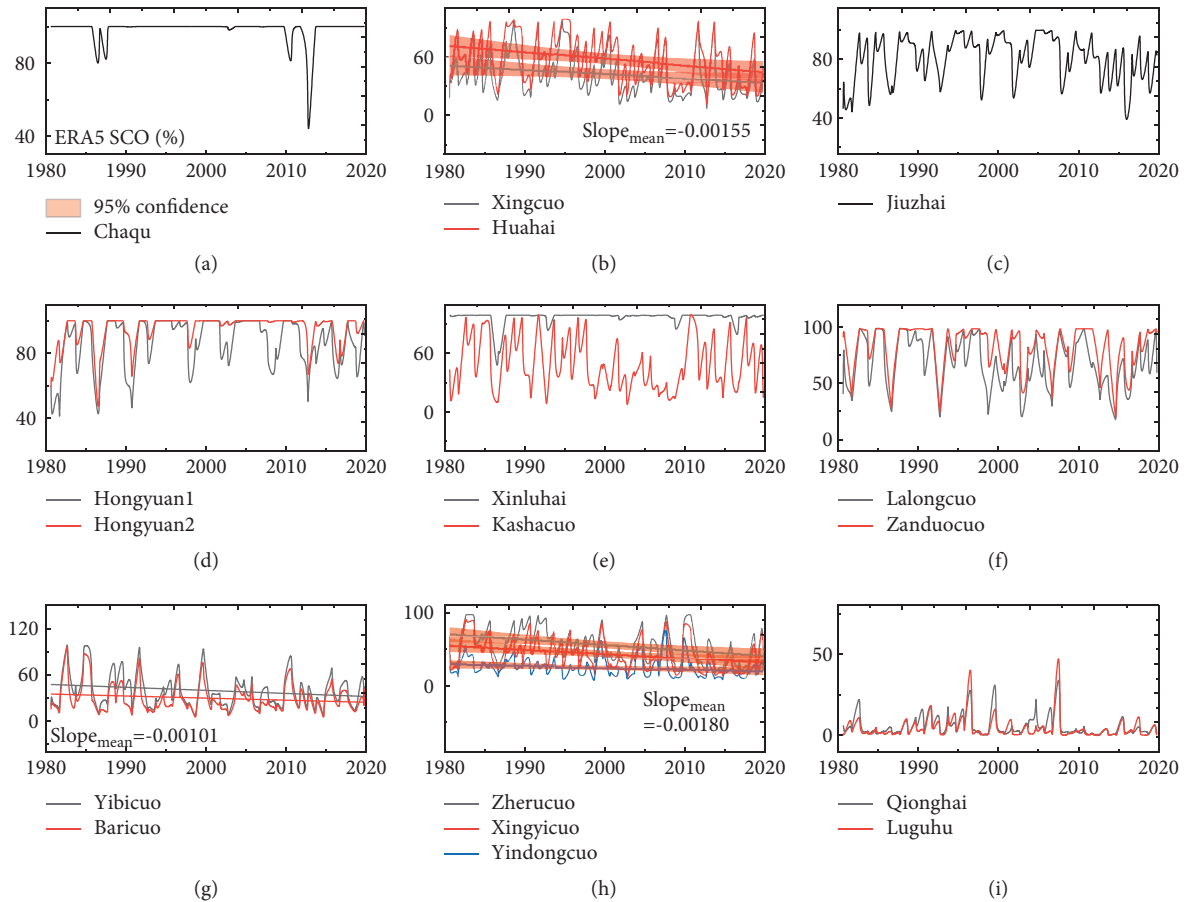
FIGURE 13: SCO change trend of the lake wetland on a site scale (2000–2020). Latitude of the lake site gradually decreased from subfigure (a) to (i). Elevation of sites (a), (d), (g), (f), and (h) are above 4500 m, elevation of sites (b), (c), and (e) are about 3000–3900 m, and elevation of site (i) is less than 3000 m.

Accordingly, we use the above-mentioned three kinds of raster to analyze EEAW's external interference by human actives based on GEE platform.

The analysis results of five plots based on the night light remote sensing imagery and population raster (Figures 15(b) and 15(c)) showed that the night light intensity of settlements and urban area appeared an upward trend; especially after 2009 (slope = 5.05/decade, $a = 0.05$), the upward trend was more obvious. This uptrend also displays that the alpine wetlands in WSCP are more seriously affected by the expansion of human settlements, even with a small population in this area. It can be seen that the populations of plot2, plot4, and plot5 have increased rapidly, and their growth rates are 93.8/decade ($a = 0.05$), 52.5/decade ($a = 0.05$), and 31.6/decade ($a = 0.05$), respectively (Figure 15(a)). Due to the low spatial resolution of the population raster data, the raster value cannot very accurately reflect the actual population distribution. We combined the demographic data of Ganzi prefecture and Aba prefecture to reanalyze the change trend of the population, and an interesting phenomenon found the urbanization rate in this area is faster than the population growth. Through field investigation (10 Aug, 2020), it is caused by rapid infrastructure construction and targeted poverty alleviation, which has accelerated the urbanization

process in this ethnic minority area dominated by Tibetan and Qiang. Additionally, the LSTs of the five wetland plots have no obvious trend change characteristics, which is consistent with the changes of farmland, especially the paddy area in this region.

## 5. Discussion

*5.1. Difference of Multiscale Analysis.* The spatial distribution and shape of alpine lake wetlands and swamp wetlands are significantly different, so we analyze the wetland ecological environment at the site scale and the plot scale, respectively. At the plot scale ($40 \times 50$ km), we analyzed changes in the ecological environment of the alpine swamp wetlands in this study. At the same time, we are also concerned about whether the scale change has an impact on the results. MODIS raster and ERA5 raster are the two-representative data (time and spatial resolution) used in this study. Therefore, the NDVI and ATP variation trends of the alpine swamp wetlands at different scales were compared and analyzed (Figure 16) in plot4 to discuss the impact of scale changes on the analysis results. Starting from the center of plot4, the NDVI and ATP in the circles with different radii were analyzed (see Figure 2 for the method), and the results are shown in Figure 16. The
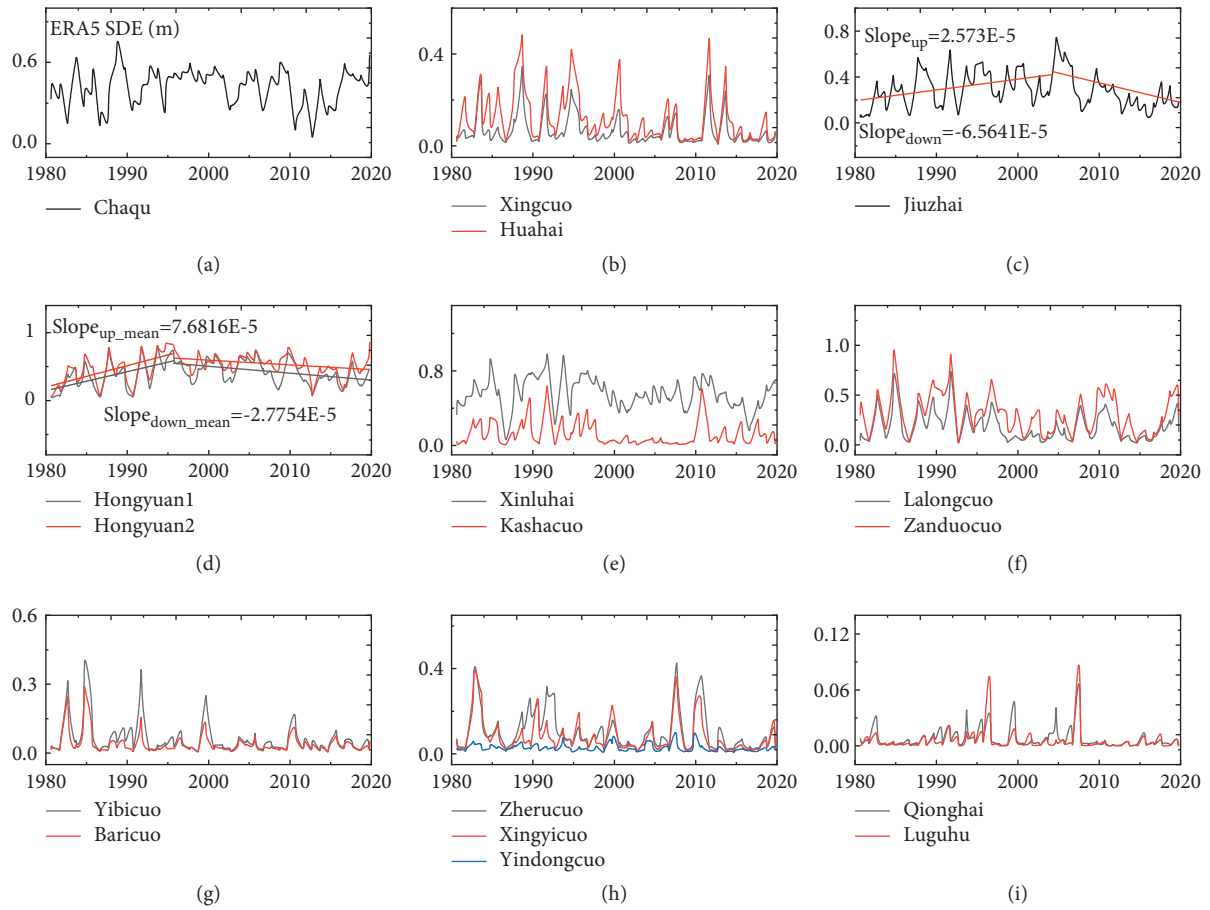
FIGURE 14: SDE change trend of the lake wetland on a site scale (2000–2020). Latitude of the lake site gradually decreased from subfigure (a) to (i). Elevation of sites (a), (d), (g), (f), and (h) are above 4500 m elevation of sites (b), (c), and (e) are about 3000–3900 m, and elevation of site (i) is less than 3000 m.
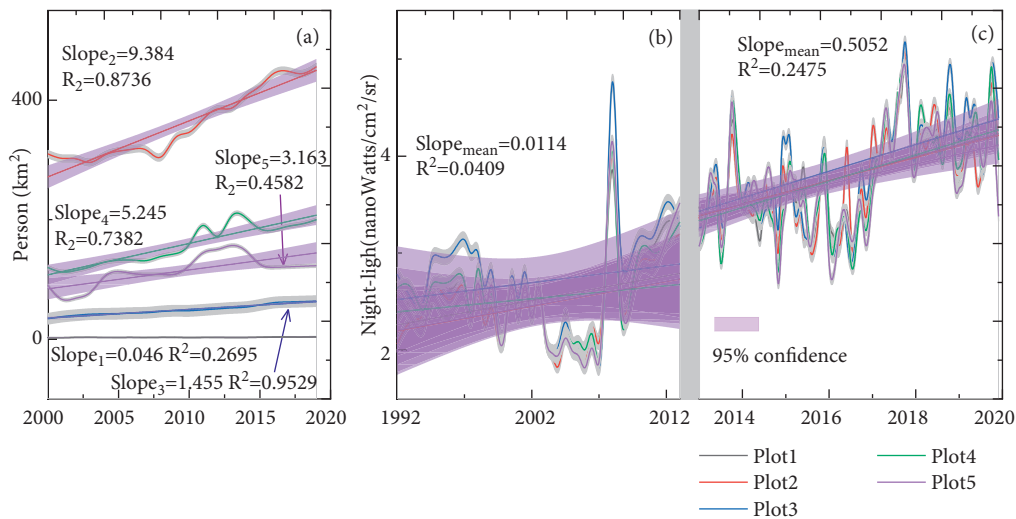


FIGURE 15: External disturbance changes trend of the swamp wetland on a plot scale. (a), (b), and (c) are the change trend of POP (2000–2020), Night-light (1992–2012), and Night-light (2012–2019), respectively.

smaller the statistical circle is, the more obvious the slope of NDVI (Figure 16(a)) increases. When $R$ is greater than 20 km, the slope does not increase significantly. In addition, the smaller the statistical scale, the greater the volatility of the analysis results. With lower resolution ATP raster, scale changes have little effect on analysis results. It can be seen that for analysts with higher resolution raster, the scale change (within a certain range) has an obvious effect on the statistical
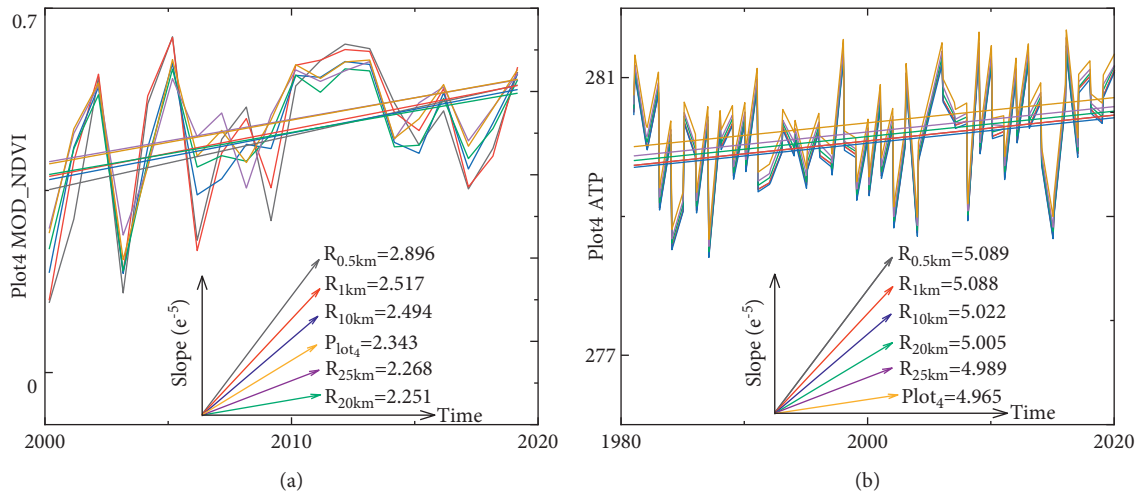
Figure 16: Slope varies with statistical scale.

results, but it is not obvious for the lower resolution raster. The analysis of the wetland ecological environment in this paper is performed on a single resolution raster (resampling and normalization), so the statistical method is scientific and reasonable. Moreover, we also want to point out that the research on the variation trend of swamp wetlands at different scales in the whole study area is also the focus of our further research in the future.

*5.2. Validation of EEAW Change.* Using the method of this article to analyze the wetland vegetation change in five plots, the wetland vegetation of high-altitude experienced an increasing trend, while it appeared a decline in low-altitude area. Especially in plot1 and plot2, the phenomenon of vegetation degradation is more obvious. Therefore, we used multiple periods Landsat images and their NDVI index to verify the vegetation changes and intensity of human activity in the two plots mentioned above. The change trend of Landsat NDVI in the past 20 years shows that the vegetation index has also declined in Zoige and Hongyuan areas. Obviously, it is consistent with the change trend of MODIS NDVI\EVI in this study. Through the analysis of the characteristics of Landsat imagery in the recent period, the main reason for the decline in NDVI is agricultural and urban expansion. Previous studies had also proved the degradation of alpine wetland meadow in Zoige area, such as the shrinkage of meadow [51], ecological degradation [20], the increase of cultivated land [52], and the tourism development [53, 54]. The validation showed that the results of vegetation dynamic and change trend are reasonable and credible in this study.

The results of raster data analysis showed that ATP in the study area showed a clear upward trend, especially in plot1, plot2, plot4, and plot5. However, the low spatial resolution of the data used made the analysis results uncertain. Therefore, we use meteorological observation data to verify the results. Specifically, the ATP observation data of the nearest meteorological station from the alpine wetland plot

was used to verify the change trend of the ERA5 ATP raster and compute the correlation between the two data in the above four plots (Figure 17). The validation results showed that the ATP of the four plots experienced an upward trend and passed the confidence test at the 0.05 level. The change trend is consistent with the previous analysis (ERA5). Due to the spatial distance and altitude difference between the meteorological observation station and the plot, there are differences in the upward trend slope and the temperature value. plot1 and plot2 are closer to their respective meteorological observation stations, so this difference is also lower.

Additionally, we also analyzed previous studies of climate change in this region to support our findings. The temperature in western Sichuan shows an increasing trend [55, 56], and the overall temperature change trend is consistent with the results of this paper. In his research, Su believes that the precipitation in WSCP has an increasing trend, but it has been declining in the past 20 years [57]. Our research also shows that the precipitation in this area has shown a downward trend in recent double decades, indicating that the analysis of climate raster dataset using this approach is credible. The snow cover of the WSCP shows a slight decrease [58]. This study confirms the description of the change trend of snow cover depth and area in this paper.

In view of the above-mentioned impacts of climate change and human activities on alpine wetlands, we use the wetland resource survey data (Table 3) in 1999, 2013, and 2021 to verify the wetland changes. By comparing the area of lake wetland, it can be found that some lake wetlands in high-latitude areas show a decreasing trend of fluctuations, such as Shiqu county, Zoige county, Luhuo county, and Dege county. This is in line with the trend of increasing temperature, decreasing precipitation, and increasing drought in this area. The area of some lake wetlands in the mid-latitude and high-altitude areas has shown an increasing trend. The climate change in this area shows an increase in temperature, an increase in precipitation, and a
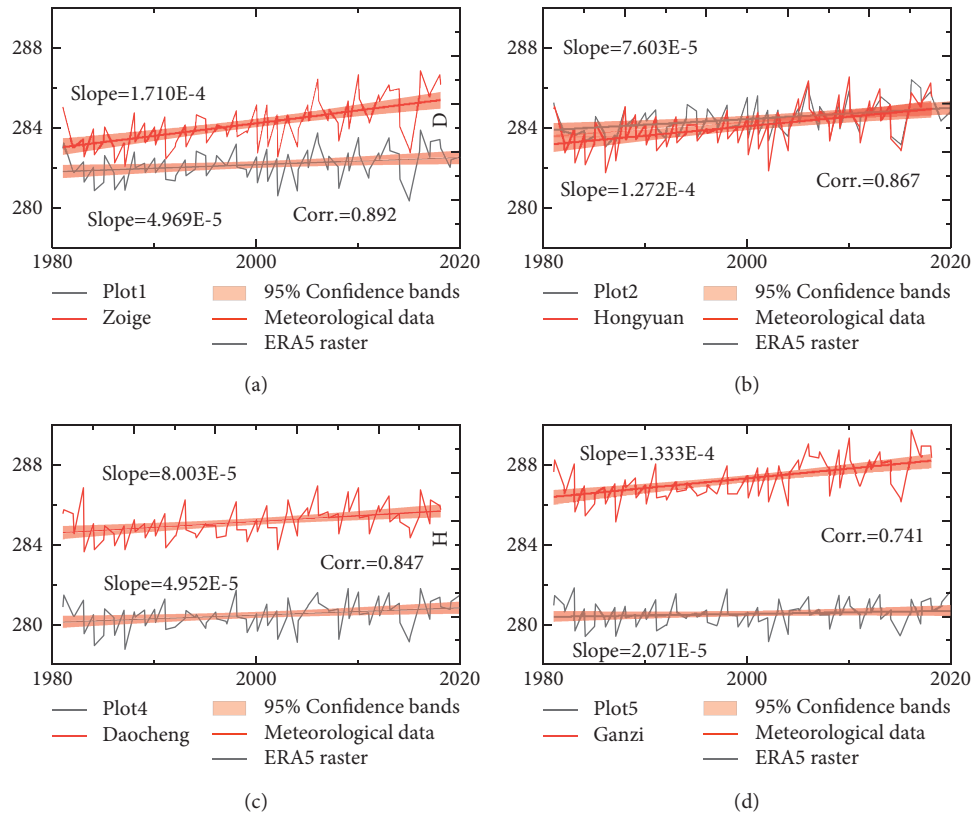
(a)

(b)

(c)

(d)

FIGURE 17: Consistency analysis of meteorological observation data and ERA5 raster.

TABLE 3: Wetland area of swamps and lakes in different periods under the same standard (hm$^2$).

| County-scale | Swamp wetland survey data | | Lake wetland survey data | | Site-scale | Lake wetland survey data | | |
|---|---|---|---|---|---|---|---|---|
| | 2013 | 2020 | 2013 | 2020 | | 1999 | 2013 | 2020 |
| Zoige | 275499.9 | 276232.9 | 2875.6 | 2836.5 | Xingcuo | 405 | 474.7 | 302.3 |
| | | | | | Huahai | 620 | 574.8 | 571.4 |
| Shiqu | 275796.5 | 276035.6 | 6483.7 | 6504.6 | Chaco | 116 | 83.6 | 61.0 |
| | | | | | Gengdi | 110 | 83.4 | 91.3 |
| | | | | | Xingyi | 680 | 730.1 | 741.8 |
| Daocheng | 24635.4 | 24674.4 | 4103.53 | 4684.4 | Yincuo | 188 | 173.8 | 179.8 |
| | | | | | Zheru | 230 | 193.5 | 197.6 |
| | | | | | Xinkai | 100 | 87.2 | 83.7 |
| Xinglong | 471437.4 | 470308.3 | 1785.9 | 1706.8 | Zanduocuo | 378 | 352.9 | 302.9 |
| Luhuo | 4568.6 | 4607.6 | 140.1 | 161.1 | Kasha | 122 | 105.3 | 83.4 |
| Dege | 18329.4 | 18368.4 | 524.7 | 545.7 | Xinluhai | 273 | 241.8 | 237.0 |
| Baiyu | 17226.5 | 17265.5 | 664.1 | 684.9 | Xiangyang | 162 | 154.3 | 162.3 |
| Batang | 5720.3 | 5759.4 | 1600.5 | 1654.3 | Yamo | 197 | 203.4 | 176.7 |
| Xichang | — | — | — | — | Qionghai | 2685 | 2644.5 | 2583.3 |
| Yanyuan | — | — | — | — | Luguhu | 2734 | 2509.8 | 2455.6 |

decrease in snow cover. It can be seen that the snow melt water has provided a good water supply to the lake wetland and swamp wetland. In low-latitude and low-altitude areas (Lugu Lake, Qionghai), the temperature increases and the precipitation decreases. Human activities have a serious impact on the area, especially the urban expansion and the rapid development of tourism. The area changes of lake wetlands can also prove the impact of climate factors and human activity on wetland changes.

5.3. Recommended Strategies for EEAW Protection. A scientific and effective wetland ecological monitoring system is very important to the protection of EEAW. Currently, the wetland ecological monitoring in WSCP is mainly in the form of establishing the nature reserves. Wetlands in WSCP are widely distributed, while there are only 7 provincial wetland nature reserves. It can be seen that it is not sufficient to conduct wetland ecological monitoring only through wetland nature reserves, so a wetland monitoring system

should be established linking the protection areas and the territories. We should conduct classified management of wetlands in western Sichuan, especially for wetlands with a small range and poor anti-interference ability, and strengthen local monitoring. With reference to the "River and Lake Chief" system implemented by the Chinese government in 2016, the task of monitoring wetland is assigned to townships, villages, and individuals. Main ecological indicators such as the area, water level, flora, and fauna of "endangered" wetlands should be continuously monitored. Additionally, surface automatic hydrological monitoring sensors should be used for rivers, lakes, and swamps that are not easy to reach and are also key monitoring region. Establish a multisource remote sensing hydrological monitoring center in western Sichuan, including small satellites, UAV, and ground fixed sensors.

Lake wetland changes are mainly driven by regional climate changes, while changes in swamps are more affected by human actives such as the development of agriculture, urban expansion, and ecotourism. Comparing the remote sensing image of typical wetlands, it can be seen that the road network density in the Zoige wetland, Haizishan wetland, and Hongyuan wetland, has increased significantly in the past 20 years. Therefore, coordinating the protection of wetland and the development of agriculture and tourism is the key work content of government departments. According to the ecological positioning of the WSCP in the NLAP outline, comprehensively analyze the resource and environmental capacity of this area, and scientifically make a plan for agriculture and tourism. For agriculture and tourism development, there should be a practical and feasible ecological compensation mechanism, especially agricultural irrigation and tourist parks. A normal artificial water replenishment program should be established, and the government should cooperate with the enterprise or individual with policy and financial support. Moreover, the government should incorporate key wetland protection and restoration projects into an important part of national economic construction.

## 6. Conclusion

This study proposed a practical and effective approach for using a big geospatial data to monitor the EEAW change on a multiscale based on cloud computing platform with an open source. The approach consists of a coupled statistical algorithm, an ecological environment monitoring index system, big geospatial dataset, and a cloud computing platform. This feasibility and effectiveness of the approach proposed has been fully assessed and proved by comparing the estimation results with previous study and field survey from an integrated multisource remote sensing image.

We used this approach to reveal the change characteristics of EEAW in WSCP, specifically including the following aspects. (1) The air temperature has shown an upward trend, and it has become more significant in the recent two decades. Precipitation in high latitudes experiences a downward trend, low latitudes-high altitudes have a slight upward trend, and the change trend has obvious north-south differentiation. (2) The evaporation has increased, and the severity of drought has also increased significantly in high latitudes. In low-latitude and high-altitude areas, the severity of drought has eased with the increase in precipitation. (3) The snow cover area has decreased, especially in the southern part of Hongyuan county, the southern section of Xinglong county, and the Haizishan region. The rate of snow melting in high-altitude areas is increasing, and the water supply of swamp wetlands in the downstream areas has been improved significantly. (4) The wetland vegetation has deteriorated significantly in Zoige county. The settlements expansion and the development of tourism have become the main factors of external interference in alpine wetlands, particularly in Zoige area and the Lugu Lake area.

In conclusion, by analyzing and discussing the change trend of the EEAW, it can be seen that we cannot be too optimistic about the ecological environment of the alpine wetland in WSCP. We should establish a scientific and effective EEAW protection strategy, especially the EEAW monitoring system and the coordination of wetland protection and economic development. As an important part of the terrestrial ecosystem, the protection of alpine wetlands can fully play the role of NEFZ in northwest Sichuan and provide a solid foundation for establishing the national ecological barrier and achieve carbon peaks in northwest Sichuan of China.

## Data Availability

The dataset is available at https://developers.google.com/earth-engine/datasets/. Note that this requires user to register with GEE.

## Conflicts of Interest

The authors declare no conflicts of interest.

## Acknowledgments

## References

[1] G. Sun, "Development and prospect of wetland science in China," *Advances in Earth Science*, vol. 15, pp. 666–672, 1992, in Chinese.

[2] Z. Sun, J. Liu, and B. Li, "The actuality, problems and sustainable utilization countermeasures of wetland resources in China," *Journal of Arid Land Resources and Environment*, vol. 20, pp. 83–88, 2006, in Chinese.

[3] Z. Zhao, Y. Zhang, L. Liu, F. Liu, and H. Zhang, "Recent changes in wetlands on the Tibetan Plateau: a review," *Journal of Geographical Sciences*, vol. 25, no. 7, pp. 879–896, 2015.

[4] S. C. Pennings, "The big picture of marsh loss," *Nature*, vol. 490, no. 7420, pp. 352-353, 2012.

[5] A. D. Lemly, R. T. Kingsford, and J. R. Thompson, "Irrigated agriculture and wildlife conservation: conflict on a global scale," *Environmental Management*, vol. 25, no. 5, pp. 485–512, 2000.

[6] R. J. McInnes, N. C. Davidson, C. P. Rostron, M. Simpson, and C. M. Finlayson, "A citizen science state of the world's wetlands survey," *Wetlands*, vol. 40, no. 5, pp. 1577–1593, 2020.

[7] "National Forestry and Grassland Administration," China's wetland area, 2018, https://www.forestry.gov.cn/main/142/20180717/144048138865928.html.

[8] National Forestry and Grassland Administration, "The second national wetland resource survey," 2014, https://www.forestry.gov.cn/main/65/content-758154.html.

[9] H. J. Wang, P. H. Peng, X. D. Kong, T. B. Zhang, and G. H. Yi, "Vegetation dynamic analysis based on multisource remote sensing data in the east margin of the Qinghai-Tibet plateau, China," *PeerJ*, vol. 7, Article ID e8223, 2019.

[10] Y. X. Yang, "New knowledge on the progress of international wetland science research and priority field and prospect of Chinese wetland science research," *Advances in Earth Science*, vol. 17, pp. 508–513, 2002, in Chinese.

[11] M. J. Hou, J. L. Gao, and J. Ge, "An analysis of dynamic changes and their driving factors in marsh wetlands in the eastern Qinghai-Tibet plateau," *Acta Prataculturae Sinica*, vol. 29, no. 1, pp. 13–27, 2020, in Chinese.

[12] K. Y. Zhao, *Chinese Swamp History*, Science Press, Beijing, China, 1st edition, 1999.

[13] L. J. Yan and W. Qi, "Lakes in Tibetan plateau extraction from remote sensing and their dynamic changes," *Acta Geoscientia Sinica*, vol. 33, pp. 65–74, 2018, in Chinese.

[14] H. F. Zhuang, Y. A. Wang, and Z. Wang, "A scientific dataset of useful plants of China," *Science Data Bank*, http://www.scidb.cn, 2021.

[15] D. A. Scott, "The black-necked cranes *Grus nigricollis* of *Ruoergai marshes*, Sichuan, China," *Bird Conservation International*, vol. 3, no. 3, pp. 245–259, 1993.

[16] T. Yao, "A comprehensive study of water-ecosystem-human activities reveals unbalancing Asian water tower and accompanying potential risks," *Chinese Science Bulletin*, vol. 64, no. 27, pp. 2761–2762, 2019.

[17] G. D. Xie, C. X. Lu, and Y. F. Leng, "Ecological assets valuation of the Tibetan plateau," *Journal of Natural Resources*, vol. 18, pp. 189–196, 2003, in Chinese.

[18] H. L. Sun, D. Zheng, T. D. Yao, and Y. L. Zhang, "Protection and construction of the national ecological security shelter zone on Tibetan plateau," *Acta Geographica Sinica*, vol. 67, pp. 3–12, 2012.

[19] Z. W. Liu, S. N. Li, W. Wei, and X. J. Song, "Research progress on alpine wetland changes and driving forces in Qinghai-Tibet plateau during the last three decades," *Chinese Journal of Ecology*, vol. 38, pp. 856–862, 2019, in Chinese.

[20] G. Shen, X. Yang, Y. Jin, B. Xu, and Q. Zhou, "Remote sensing and evaluation of the wetland ecological degradation process of the Zoige plateau wetland in China," *Ecological Indicators*, vol. 104, pp. 48–58, 2019.

[21] Y. Guang, Z. B. Hu, J. F. Dong, C. Lu, and Y. Zhen, "The developmental trend and influencing factors of aeolian desertification in the Zoige Basin, eastern Qinghai–Tibet plateau," *Aeolian Research*, vol. 19, pp. 275–281, 2015.

[22] R. B. Harris, "Rangeland degradation on the Qinghai-Tibetan plateau: a review of the evidence of its magnitude and causes," *Journal of Arid Environments*, vol. 74, no. 1, pp. 1–12, 2010.

[23] X. M. Kang, Y. B. Hao, X. Y. Cui, H. Chen, S. X. Huang, and Y. Du, "Variability and changes in climate, phenology, and gross primary production of an alpine wetland ecosystem," *Remote Sensing*, vol. 8, no. 391, pp. 1–14, 2016.

[24] N. N. Zhao, S. Gou, B. B. Zhang, Y. L. Yu, and S. J. Han, "Changes in pan evaporation and their attribution to climate factors in the Zoige alpine wetland, the eastern edge of the Tibetan plateau (1969–2014)," *Water*, vol. 9, no. 971, pp. 1–14, 2017.

[25] M. J. Hou, J. Ge, J. L. Gao et al., "Ecological risk assessment and impact factor analysis of alpine wetland ecosystem based on LUCC and boosted regression tree on the Zoige plateau, China," *Remote Sensing*, vol. 12, no. 368, pp. 1–22, 2020.

[26] B. Z. Carlson, M. Hebert, C. V. Reeth, M. Bison, I. Laigle, and A. Delestrade, "Monitoring the seasonal hydrology of alpine wetlands in response to snow cover dynamics and summer climate: a novel approach with sentinel-2," *Remote Sensing*, vol. 12, pp. 1–19, 2020.

[27] W. L. Li, P. F. Xue, C. L. Liu, H. P. Yan, G. F. Zhu, and Y. P. Cao, "Monitoring and landscape dynamic analysis of alpine wetland area based on multiple algorithms: a case study of Zoige plateau," *Sensors*, vol. 20, no. 7315, pp. 1–19, 2020.

[28] J. Y. Wang, H. Z. Sun, J. N. Xiong et al., "Dynamics and drivers of vegetation phenology in three-river headwaters region based on the google earth engine," *Remote Sensing*, vol. 13, no. 13, p. 2528, 2021.

[29] A. Savitzky and M. J. E. Golay, "Smoothing and differentiation of data by simplified least squares procedures," *Analytical Chemistry*, vol. 36, no. 8, pp. 1627–1639, 1964.

[30] Google earth engine, "A planetary-scale platform for Earth science data & analysi," 2022, https://earthengine.google.com/.

[31] European earth server, "Planetary-Scale Earth Data-cube Federation," 2020, https://www.earthserver.eu/index.php#about.

[32] Amazon Web Services, "Registry of open data on AWS," 2020, https://registry.opendata.aws/.

[33] N. Gorelick, M. Hancher, M. Dixon, S. Ilyushchenko, D. Thau, and R. Moore, "Google earth engine: planetary-scale geospatial analysis for everyone," *Remote Sensing of Environment*, vol. 202, pp. 18–27, 2017.

[34] H. Theil, "A rank-invariant method of linear and polynomial regression analysis," in *Henri Theil's Contributions to Economics and Econometrics*, B. Raj and J. Koerts, Eds., vol. 23, pp. 348–381, Springer, Berlin, Germany, 1992.

[35] H. S. Chu, S. Venevsky, C. Wu, and M. H. Wang, "NDVI-based vegetation dynamics and its response to climate changes at Amur-Heilongjiang River Basin from 1982 to 2015," *Science of the Total Environment*, vol. 650, pp. 2051–2062, 2019.

[36] Z. J. Gu, X. W. Duan, Y. D. Shi, Y. Li, and X. Pan, "Spatiotemporal variation in vegetation coverage and its response to climatic factors in the Red River Basin, China," *Ecological Indicators*, vol. 93, pp. 53–64, 2018.

[37] Z. G. Tang, J. H. Ma, H. H. Peng, S. H. Wang, and J. F. Wei, "Spatiotemporal changes of vegetation and their responses to temperature and precipitation in upper Shiyang Rriver Basin," *Advances in Space Research*, vol. 60, pp. 969–979, 2018.

[38] M. Gocic and S. Trajkovic, "Analysis of changes in meteorological variables using mann-kendall and Sen's slope estimator statistical tests in Serbia," *Global and Planetary Change*, vol. 100, pp. 72–182, 2013.

[39] S. G. Yavuz, "Multiple sen-innovative trend analyses and partial mann-kendall test," *Journal of Hydrology*, vol. 566, pp. 685–704, 2018.

[40] O. Morell and R. Fried, "On nonparametric tests for trend detection in seasonal time series," in *Statistical Inference, Econometric Analysis and Matrix Algebra*, B. Schipp and W. Kräer, Eds., pp. 19–39, Springer, Berlin, Germany, 2009.

[41] T. Pohlert, "Non-parametric trend tests and change-point detection," 2020, https://cran.r-project.org/web/packages/trend/vignettes/trend.pdf.

[42] P. K. Sen, "Estimates of the regression coefficient based on kendall's tau," *Journal of the American Statistical Association*, vol. 63, pp. 1379–1389, 2012.

[43] "Google developers-tutorial," 2022, https://developers.google.com/earth-engine/tutorials/community/nonparametric-trends#mann-kendall_trend_test.

[44] J. Christopher, V. Hein, A. Galy et al., "Post-glacial climate forcing of surface processes in the Ganges–Brahmaputra river basin and implications for carbon sequestration," *Earth and Planetary Science Letters*, vol. 478, pp. 89–101, 2017.

[45] G. Gan, Y. Liu, and G. Sun, "Understanding interactions among climate, water, and vegetation with the Budyko framework," *Earth-Science Reviews*, vol. 212, Article ID 103451, 2021.

[46] X. Fan, Y. Liu, G. Gan, and G. Wu, "SMAP underestimates soil moisture in vegetation-disturbed areas primarily as a result of biased surface temperature data," *Remote Sensing of Environment*, vol. 247, Article ID 111914, 2020.

[47] A. K. Abdulla, R. Shahinoor, A. F. Abdullah, M. H. Mohammad, and I. Muhaiminul, "Modelling future land use land cover changes and their impacts on land surface temperatures in Rajshahi, Bangladesh," *Remote Sensing Applications: Society and Environment*, vol. 18, Article ID 100314, 2020.

[48] T. V. Ramachandra, S. Bharath, and N. Gupta, "Modelling landscape dynamics with LST in protected areas of Western Ghats, Karnataka," *Journal of Environmental Management*, vol. 206, pp. 1253–1262, 2018.

[49] W. Wang, A. Samat, J. Abuduwaili, and Y. Ge, "Quantifying the influences of land surface parameters on LST variations based on GeoDetector model in Syr Darya Basin, Central Asia," *Journal of Arid Environments*, vol. 186, Article ID 104415, 2021.

[50] T. Pan, C. Zhang, W. Kuang, G. Luo, G. Du, and Z. Yin, "Large-scale rain-fed to paddy farmland conversion modified land-surface thermal properties in cold China," *Science of the Total Environment*, vol. 722, Article ID 137917, 2020.

[51] Z.-W. Li, Z.-Y. Wang, G. Brierley, T. Nicoll, B.-Z. Pan, and Y.-F. Li, "Shrinkage of the Ruoergai swamp and changes to landscape connectivity, Qinghai-Tibet plateau," *Catena*, vol. 126, pp. 155–163, 2015.

[52] X. D. Rong, T. Bo, T. Kun, and Y. Yang, "Landscape patterns and their changes in Sichuan Ruoergai wetland national nature reserve," *Acta Ecologica Sinica*, vol. 30, pp. 27–32, 2010.

[53] J. L. Chen, "Analysis on vegetation change and driving factors in the Alpine plateau of Zoige," Master Thesis, Sichuan Normal University, Chengdu, China, 2018.

[54] J. Bian, A. Li, Z. Zhang et al., "Monitoring fractional green vegetation cover dynamics over a seasonally inundated alpine wetland using dense time series HJ-1A/B constellation images and an adaptive endmember selection LSMM model," *Remote Sensing of Environment*, vol. 197, pp. 98–114, 2017.

[55] H. J. Zhang, "A study on the characteristics of climate change on northwestern Sichuan plateau," *Journal of Southwest University (Natural Science Edition)*, vol. 36, pp. 148–156, 2014, in Chinese.

[56] C. Y. Li, "Study on dry and wet climate changes in the valleys of the Hengduan mountains in western Sichuan in Recent 59 Years," Master Thesis, Sichuan Normal University, Chengdu, China, 2020.

[57] Y. Su, W. S. Mao, and C. X. Shi, "Regional characteristics of summer precipitation in southwest China in recent 60 years," *Journal of Chengdu University of Information Technology*.vol. 35, pp. 560–565, 2020, in Chinese.

[58] D. J. Zhong, M. X. Sun, and Y. Zhang, "Spatio-temporal variation and influencing factors of snow cover in west Sichuan plateau 2001 to 2020," *Journal of Arid Land Resources and Environment*, vol. 35, pp. 111–118, 2021, in Chinese.